Recent Developments in the Experimental Investigations of Relaxations in Pharmaceuticals by Dielectric Techniques at Ambient and Elevated Pressure

Katarzyna Grzybowska,[1,2] Simone Capaccioli,[3,4] and Marian Paluch[1,2,*]

[1] *Institute of Physics, University of Silesia, ul. Uniwersytecka 4, 40-007 Katowice, Poland*
[2] *Silesian Center for Education and Interdisciplinary Research, ul. 75 Pułku Piechoty 1a, 41-500 Chorzów, Poland*
[3] *Dipartimento di Fisica, Universita` di Pisa, Largo Bruno Pontecorvo 3, I-56127, Pisa, Italy*
[4] *CNR-IPCF, Largo Bruno Pontecorvo 3, I-56127, Pisa, Italy*

* Corresponding author's e-mail: marian.paluch@us.edu.pl

Abstract

In recent years, there is a growing interest in improving the physicochemical stability of amorphous pharmaceutical solids due to their very promising applications to manufacture medicines characterized by a better water solubility, and consequently by a higher dissolution rate than those of their crystalline counterparts. In this review article, we show that the molecular mobility investigated both in the supercooled liquid and glassy states is the crucial factor required to understand molecular mechanisms that govern the physical stability of amorphous drugs. We demonstrate that pharmaceuticals can be thoroughly examined by means of the broadband dielectric spectroscopy, which is a very useful experimental technique to explore different relaxation processes and crystallization kinetics as well. Such studies conducted in the wide temperature and pressure ranges provide data needed in searching correlations between properties of molecular dynamics and crystallization process, which are aimed at developing effective and efficient methods for stabilizing amorphous drugs.

Graphical abstract

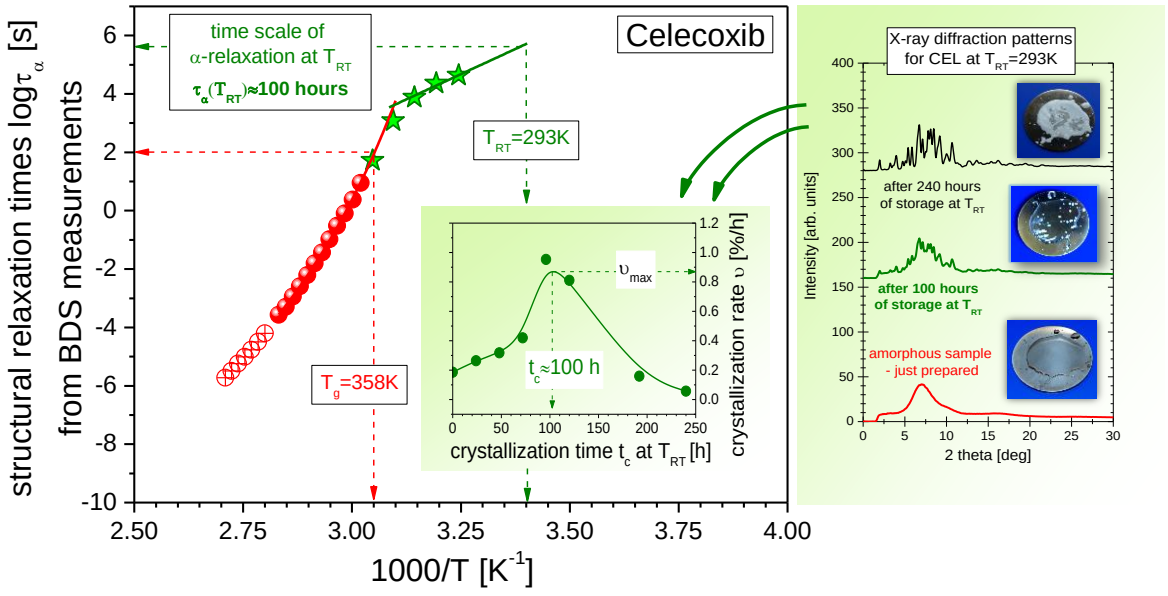

Keywords
broadband dielectric spectroscopy, amorphous drugs, physical stability, molecular mobility, dielectric relaxations, crystallization, elevated pressure

1. Introduction

Nowadays, many active pharmaceutical ingredients (APIs) are prepared in the crystalline form due to their several advantages. First of all, crystalline pharmaceuticals are thermodynamically stable, and consequently, their physicochemical properties do not change even during a long-term storage. Moreover, it is relatively easy to develop repeatable ways of synthesis and analysis of crystalline APIs. Unfortunately, many crystalline drugs are poorly water soluble. This is an extremely disadvantageous feature of crystalline forms of APIs because solubility is one of the most important physicochemical properties in pharmaceutical products design. The scale of this problem is huge, because more than 75% of drug candidates and 40% of the marketed drugs are poorly soluble in water [1,2], and consequently their bioavailability is strongly limited. A promising way to overcome the drawback is to transform crystalline pharmaceuticals characterized by a long-range translational order to their structurally disordered non-crystalline counterparts (amorphous solids), which may exhibit only a short-range order. The amorphous pharmaceutical solids due to their higher internal energy are often characterized by a better bioavailability than their crystalline counterparts. It is established that solubility and dissolution rate in water are orders of magnitude greater than their crystalline counterparts [3,4,5,6,7,8,9,10]. Unfortunately, the amorphous APIs are thermodynamically unstable systems and may even quickly return to their thermodynamically stable crystalline forms [11,12,13,14], which can happen during manufacturing, storage, or dissolution (administration).

To gain a better insight into the physical instability of amorphous drugs, the study of *the glass transition* (from liquid to glass or *vice versa*) are of special importance. The liquid-glass transition can occur upon isobaric cooling (or under isothermal compression) of a liquid when the time scale of molecular motions responsible for structural rearrangements becomes longer than the time scale of the experiment. As a result, the structural relaxation toward equilibrium is arrested below the glass transition temperature T_g (or above the glass transition pressure P_g) and the system is in the glassy state. [15]. This transformation can only be observed if nucleation is suppressed, for example, by sufficiently rapid cooling of a liquid [16]. Investigations of physical phenomena near the glass transition give us valuable information on two states in which the drugs are unstable and can recrystallize, i.e., (*i*) *the glassy state* – a

thermodynamically non-equilibrium amorphous solid state and (*ii*) *the supercooled liquid* – a thermodynamically metastable liquid state in the temperature range between T_g and the melting temperature T_m. [16,17] It should be noted that the glass transition and related phenomena are still intensively studied despite more than the half century research in this field. Even the complex nature of the glass transition is continuously under discussion, because the phenomenon falls outside the thermodynamic definitions of the first-order or the second-order phase transitions due to its kinetic character that for instance reflects in the dependence of the glass transition temperature T_g on the experiment (cooling or heating) rate. Nevertheless, a progress of physical, chemical, and material sciences made in this research area [16,17,18,19,20] enabled to develop pharmaceutical studies focused on amorphous APIs. Especially, a lot of effort has been put into better understanding the key factors that govern the recrystallization process in both the supercooled liquid and glassy states as well as finding efficient methods for stabilization of the amorphous forms of drugs.

In order to determine the amorphous solid stability, some thermodynamic properties, e.g., the configurational entropy (S_{conf}), the configurational enthalpy (H_{conf}), and the configurational Gibbs free energy (G_{conf}), have been thoroughly analyzed [21,22,23,24]. Among the configurational quantities (considered respectively as the entropic barrier, the enthalpic driving force, and the overall thermodynamic driving force for crystallization), S_{conf} has been found to be useful for predicting the physical stability of amorphous drugs and some correlations have been established between S_{conf} (or H_{conf}) and the tendency of amorphous materials to recrystallization [25,22,26,21]. Nevertheless, it has been realized that the investigations of only the thermodynamic factors are insufficient to completely solve the problems related to the physical stability of amorphous APIs, because the macroscopic thermodynamic quantities do not give us a needed insight into molecular mechanisms that govern the recrystallization process. Therefore, probably the most relevant factor, which should be studied to reliably predict the tendency of amorphous drugs to recrystallization, and consequently, to considerably contribute to the development of the effective and efficient methods for stabilization of the amorphous APIs, is their molecular mobility [27,28,29,30,31,11]. The search for proper correlations between the molecular mobility of amorphous solids and their physical stability is highly complicated, because pharmaceutical materials are often characterized by complex molecular structures of different configurational topology and a variety of intra- and intermolecular interactions, including specific interactions such as hydrogen bonds of different strength and electrostatic forces. As a result, the glass-forming pharmaceutical materials usually exhibit complex molecular mobility reflected in

several relaxation processes of different nature, which can be distinguished by their properties including their dependence on temperature and pressure. In this context, an important and fervently debated issue is an unambiguous answer to the question: *Which kind of molecular mobility of different time scales, reflected in the structural (global) relaxation associated with the glass transition or different secondary (local) relaxations, can be responsible for the recrystallization of amorphous drugs*?

To study the molecular mobility in both the supercooled liquid and glassy states (in which the time scales of different relaxation processes span an enormously wide range of more than 10 orders of magnitude [32], the most useful experimental methods are those which enable to explore the complex molecular motions with high resolution in the wide range of their time scales and under different thermodynamic conditions. Although there are several measurement techniques that can be exploited to investigate molecular dynamics (such as nuclear magnetic resonance (NMR), temperature modulated differential scanning calorimetry (TMDSC), thermally stimulated depolarization current (TSDC), quasielastic neutron scattering (QENS), positron annihilation lifetime spectroscopy (PALS), light scattering, and mechanical spectroscopy), the broadband dielectric spectroscopy (BDS) gives us the best possibility to determine time scales of molecular motions of pharmaceuticals in the glassy and liquid states. BDS measurements can be carried out in the wide range of temperatures and pressures over a broad frequency band up to 18 decades (*ca.* from mHz to THz), which enable to distinguish the global and local molecular motions characterized by their time scales that can change up to 18 orders of magnitude. In addition, the BDS techniques can be easily implemented, because the high quality BDS spectrometers readily available on the market are easy to operate and provide high accuracy experimental data at low costs of measurements (e.g., deuteration of samples is not necessary in contrast to NMR). In recent years, a considerable progress has been made in studies at elevated pressure by means of BDS.[19,18,33,34,35,36,37] It resulted in gaining a better insight into the molecular origin of dielectric relaxation processes near the glass transition as well as the compression effect on the physical stability of amorphous APIs, which is significant for instance during the tableting process [38,12,39,40,41].

In this review article, we present recent advances in understanding the tendency of amorphous APIs to recrystallization, which have been made with the aim of enhancing the physical stability of amorphous drugs by studying different kinds of molecular mobility in both the supercooled liquid and glassy states at ambient and elevated pressure by means of the BDS techniques.

2. Idea of the Broadband Dielectric Spectroscopy (BDS) and Relaxation Processes

The dielectric spectroscopy is based on the interactions of the electric dipole moment and charges of a material sample with an external electric field applied to the sample. This experimental method enables to measure the response of the examined material (polar dielectrics) to the applied alternating electric field **E**(ω) in the wide frequency range $f = \omega/2\pi$ *ca.* from 10^{-5} to 10^{11} Hz (which can be extended to about 10^{13} Hz by employing THz measurement techniques). As a result, in the frequency domain, one can explore the following phenomena occurring in the sample [42]:

- dielectric dispersion $\varepsilon'(\omega)$ and absorption $\varepsilon''(\omega)$ caused by dipoles relaxation (resulting from reorientational motions of molecular dipoles), which are represented by the complex dielectric permittivity $\varepsilon^*(\omega) = \varepsilon'(\omega) - i\varepsilon''(\omega)$;
- electrical conduction originating from the translational motions of electric charges (ions, electrons), which can be described by (*i*) the complex conductivity, $\sigma^*(\omega) = \sigma'(\omega) + i\sigma''(\omega)$, related to the complex permittivity by the equation, $\sigma^*(\omega) = i\omega\varepsilon_0\varepsilon^*(\omega)$, where ε_0 is the vacuum permittivity or (*ii*) the complex electrical modulus, $M^*(\omega) = M'(\omega) + iM''(\omega)$, related to the complex dielectric permittivity as follows $M^*(\omega) = 1/\varepsilon^*(\omega)$.

In the dielectric experiment, the investigated material is placed in a measurement capacitor (see Fig.1), to which an alternating voltage $U^*(\omega)$ is applied by a generator (typically a sine wave voltage). As a result, the alternating electric field **E**(ω) is generated between the capacitor plates, which is the external field acting on the sample. Then, the impedance analyzer determines the complex impedance of the sample, $Z_s^*(\omega) = U_s^* / I_s^*$, by measuring the complex voltage $U_s^*(\omega)$ between the plates of the sample capacitor as well as the current $I_s^*(\omega)$[43].

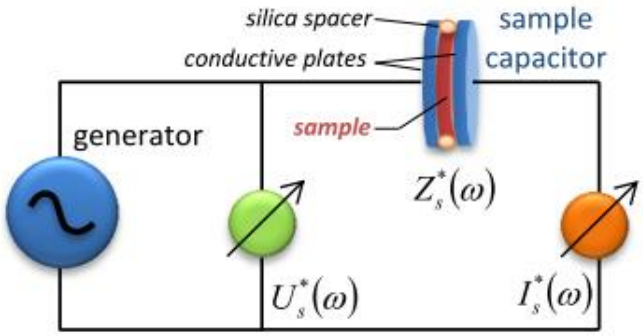

Fig. 1 Diagram of the typical impedance analyzer, which illustrates the principle of the dielectric measurements in the frequency domain.

The basic quantity measured by broadband dielectric spectrometers (equipped with the impedance analyzer) is the complex electrical impedance $Z^*(\omega)$, which allows to derive the other complex quantities such as $\varepsilon^*(\omega), \sigma^*(\omega)$, and $M^*(\omega)$. The BDS apparatuses can usually provide the measurement data in each mentioned complex representation. For instance, the complex dielectric permittivity $\varepsilon^*(\omega)$ of the sample can be found from the ratio of the complex capacitance of the capacitor filled with the investigated material $C_s^*(\omega)$ and the capacitance of the empty capacitor C_0, i.e., $\varepsilon^*(\omega) = C_s^*(\omega)/C_0$, where $C_s^*(\omega)$ is related to the sample impedance as follows, $C_s^*(\omega) = -i/\omega Z_s^*(\omega)$. Therefore, the dielectric function $\varepsilon^*(\omega)$ of the material can be established from the sample impedance $Z_s^*(\omega)$ measurements in the following way, $\varepsilon^*(\omega) = \varepsilon'(\omega) - i\varepsilon''(\omega) = -i/\omega Z_s^* C_0 = -i/\omega C_0 (U_s^*/I_s^*)$, where the capacitance of the empty capacitor C_0 depends on its geometry (e.g., $C_0 = \varepsilon_0 S/d$ for a parallel capacitor, where d is the distance between the capacitor plates and S is the area of one plate).

If the molecular mobility of a material need to be investigated in the extremely wide frequency range (10^{-5} – 10^{13}) *Hz*, which corresponds the relaxation time range (10^{4} – 10^{-14}) s, a few experimental dielectric techniques have to be employed. The frequency-response analysis, AC-bridge methods, coaxial-line reflectometry, network analysis (coaxial-line transmition) enable to conduct the dielectric study in the frequency domains shown in Fig. 2. The measurement techniques are described in details in Refs. [42,43,44]. In the last decade, the frequency range typically scanned by the different BDS techniques has been extended to THz frequencies (10^{11} – 10^{13}) *Hz*. One of milestones in the THz technology is the THz time domain spectroscopy (THz-TDS) [45]. By means of this technique, the absorption coefficient

and the refractive index of materials are directly measured, which are subsequently used to determine the dispersion $\varepsilon'(\omega)$ and the absorption $\varepsilon''(\omega)$ [46].

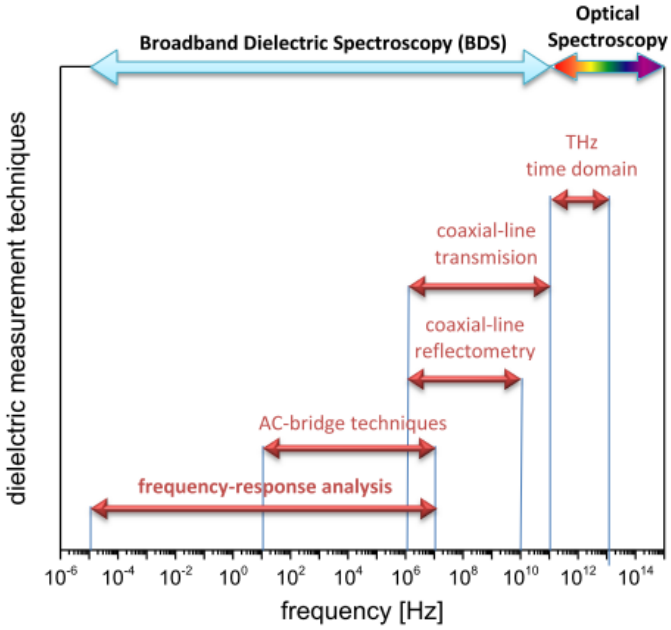

Fig. 2 Dielectric measurement techniques typically exploited in the frequency range from 10^{-5} to 10^{11} Hz (extended to the THz frequency domain). The broadband dielectric spectroscopy frequency range reaches the low frequency limit of the optical spectroscopy.

Nowadays, using commercial spectrometers, the accurate dielectric measurements of various liquid and solid materials can be performed not only over the broad frequency bands but also in the wide temperature and pressure ranges. It makes the dielectric spectroscopy useful in many fields of science and technology, including pharmaceutics [42] to study (*i*) the molecular dynamics of liquids, liquid crystals, glasses, disordered crystals, (*ii*) charge transport in ionic liquids, semiconductors, organic crystals, ceramics, etc., (*iii*) structural material properties like phase compositions. The BDS can be also applied to monitor chemical reactions (e.g., polymerization, tautomerization of drugs, mutarotation of sugars) and phase transitions (e.g., crystallization, vitrification, evaporation). In case of pharmaceutical applications, the BDS is undoubtedly a powerful method to investigate different kinds of molecular mobility of drugs in various thermodynamic conditions (in both the supecooled liquid and glassy states) in search of the correlations between the complex molecular mobility and the physical instability of the amorphous solid forms of the drugs.

Dielectric relaxation processes and related molecular motions

Depending on molecular structure of examined systems as well as thermodynamic conditions (temperature T and pressure P), different relaxation processes can be observed in

the dielectric spectra of investigated materials. A common feature of the glass forming liquids is a global relaxation process (called structural α-relaxation), which can be measured in the liquid state (at $T>T_g$). In case of low molecular weight materials, the α-relaxation reflects reorientations of entire molecules, which are considered to have a cooperative nature, i.e., each molecule requires some reorientations of surrounding molecules for its reorientation. For polymers, the structural α-relaxation is also called segmental relaxation, because it is related to some segmental motions in polymer chains, which result in conformational changes of the macromolecules. The structural α-relaxation reveals usually as a broad and asymmetric peak in the dielectric loss spectra $\varepsilon''(\omega)$, the magnitude of which is significantly larger than that for other relaxation processes (see Fig. 3). The characteristic time scale of any relaxation process (including α-relaxation) is its relaxation time τ, which can be determined from dielectric spectra using the equation, $\tau=1/2\pi f_{max}$, where f_{max} is the frequency at which the maximal dielectric loss of the relaxation process is observed (i.e., at the maximum of the loss peak of the relaxation process). Upon decreasing temperature or increasing pressure, the structural relaxation peaks shift towards lower frequencies (i.e., longer time scales). It indicates that molecular motions reflected in the α-relaxation become slower (i.e., their time scale τ_α becomes longer). The structural relaxation time τ_α rapidly increases (over several orders of magnitude in a narrow range of temperatures or pressures) when a liquid is approaching its glass transition upon isobaric cooling or isothermal squeezing of the liquid. This behavior is regarded as one of the main characteristics of the liquid-glass transition. A liquid achieves the glassy state at some characteristic time scale τ_g, which is often arbitrarily assumed to correspond the structural relaxation time τ_α=100s. At sufficiently low temperatures (below the glass transition temperature T_g) or high pressures (above the glass transition pressure P_g), the structure of liquid becomes "frozen" and the system reaches the glassy state. Since the molecular mobility reflected in the structural relaxation is very slow in the glassy state, the experimental detection of α-relaxation in glassy materials requires extremely time-consuming measurements and only some predictions of the α-relaxation times are performed. Therefore, in the glassy state, usually only secondary relaxations resulting from some local molecular motions, which are characterized by time scales considerably shorter than that of α-relaxation, are experimentally measured by means of BDS.

The local motions of different nature are reflected in different secondary relaxations (denoted by β, γ, δ, *etc.*), which in general have either inter- or intermolecular origin. Among them, the fast local reorientations of entire molecules reflected in the so called Johari -

Goldstein (JG) process are of particular interest. Independently of the heterogeneous [47,48] and homogeneous [49] pictures, which are still discussed for molecular mechanisms of the JG process, this intermolecular secondary β-relaxation is regarded as a precursor of the molecular mobility of the cooperative α-relaxation. It means that such small-angle reorientations of entire molecules are to lead to the global α-relaxation. The JG secondary relaxation is postulated to be a universal feature of all glass formers, although a well-resolved β-relaxation dielectric loss peak cannot be observed for some materials, for which only an additional flank (so called "excess wing") is present on the high frequency side of the α-relaxation peak. As a result of the fervent debate, the excess wing has been suggested by Johari and Pathmanathan[50] as a high-frequency flank of the β-relaxation peak hidden underneath the dominating structural α-relaxation peak. This very likely interpretation has been later confirmed by performing high pressure BDS measurements [51]. During isothermal compression, the excess wing becomes more and more prominent, and then a well separated β-relaxation peak can be distinguished in dielectric spectra at sufficiently high pressure. On the other hand, an isobaric increase in temperature leads to a growth of the coupling between α- and β-relaxations, and consequently to a merging of the processes well above T_g, which occurs at a time scale ($\tau_\beta=\tau_\alpha$) usually less than 10^{-6}s.

In dielectric spectra of many glass formers, besides the structural α-relaxation and the intermolecular JG β-relaxation, other faster secondary processes can be observed, which are denoted by γ, δ, *etc.* according to their decreasing time scales (i.e., relaxation times $\tau_\beta > \tau_\gamma > \tau_\delta$ *etc.*). The local motions reflected in the secondary (γ, δ, *etc.*) processes usually have an intramolecular character (e.g., reorientations of some parts of molecules) and are classified as non-JG relaxations. A more detailed classification of secondary relaxations, which additionally involves pseudo-JG processes is given in Ref.[52]. The intramolecular origin of non-JG secondary relaxations can be well verified in high pressure experiments, because the non-JG processes are practically pressure independent in contrast to the intermolecular secondary JG relaxation. A useful tool to identify the JG- and non-JG secondary processes constitutes the extended coupling model formulated by K.L. Ngai [52], which is presented in Section 3.2.

The briefly discussed structural and secondary relaxations do not exhaust all processes that reveal in dielectric spectra. For polymers, the so called "normal mode", which originates from the sum of the segmental dipole moments parallel to the polymer chain backbone [53], is often observed in the frequency range lower than that typical for α-relaxation. For some materials (e.g. monoalcohols), also at low frequencies, a Debye peak can appear, which is

suggested to reflect a formation of chain-like structures. Moreover, in the low frequency limit, a DC conduction, which originates from the translational motions of electric charges (ions), contributes to each dielectric absorption spectra ε"(ω). In the THz frequency range, a few processes have been identified, including some fast processes related to librational-vibrational motions and the so called "boson peak", the molecular origin of which is still not fully understood.

The entire dielectric spectra (both the dispersion $\varepsilon'(\omega)$ and the absorption $\varepsilon''(\omega)$) measured in the broad frequency range are most often analyzed as a superposition of the individual relaxation processes (i.e., each of them is described by the separate Havriliak-Negami (HN) function [54, 55]) and the DC conduction term:

$$\varepsilon^*(\omega) = \varepsilon'(\omega) - i\varepsilon''(\omega) = -i\left(\frac{\sigma_{DC}}{\varepsilon_0 \omega}\right)^N + \varepsilon_\infty + \sum_k \frac{\Delta\varepsilon_k}{\left[1 + (i\omega\tau_k)^{1-\alpha_k}\right]^{\beta_k}}, \quad (1)$$

where σ_{DC} is the DC conductivity, N most frequently equals 1, k numbers dielectric processes identified in a dielectric spectrum. The fitting parameter τ_k of Eq. (1) is commonly considered as the relaxation time of k-process, although τ_k slightly differ from that determined at the frequency f_{max} at which the maximum dielectric loss of the k-process occurs [42]. In general, asymmetric loss peaks (usually observed for α-relaxation) can be fitted to the HN function. Nevertheless, the fitting parameters α_k and β_k of Eq. (1) range as follows $0 \le \alpha_k < 1$ and $0 < \beta_k \le 1$, giving the possibility to describe also symmetric peaks by the simple Debye function (for β_k=1 and α_k=0) and the Cole-Cole (for β_k=1 and $0 < \alpha_k < 1$) function [56] that is useful in fitting broad symmetric peaks often detected for secondary dielectric processes.

The thermodynamic evolution of the time scales τ_k of the relaxation processes can be described by various models. The experimental temperature dependences of structural relaxation times in the supercooled liquid state, τ_α(T), are most commonly parametrized by an empirical Vogel-Fulcher-Tamman (VFT) equation [57,58,59,60]

$$\tau_\alpha = \tau_0 \exp\left(\frac{DT_0}{T - T_0}\right), \quad (2)$$

where τ_0, T_0, and D are fitting parameters. The VFT equation finds a justification in the Adam-Gibbs (AG) theory [61] which has become a reference very often invoked in studies devoted to the understanding of mechanisms that govern the vitrification of supercooled liquids. An extended VFT equation (discussed in Section 3.1.2.1) based on the extended Adam-Gibbs model is used to predict the dependence τ_α(T) in the glassy state.

The experimental temperature dependences of secondary relaxation times (τ_β, τ_γ, *etc.*) in the glassy state are commonly fitted to the Arrhenius equation:

$$\tau(T) = \tau_\infty \exp\left(\frac{\Delta E}{k_B T}\right), \tag{3}$$

where τ_∞ is the pre-exponential factor, ΔE is the energy barrier for examined secondary process, and k_B is the Boltzmann constant. In the liquid state, the determination of secondary relaxation times from dielectric spectra is usually very difficult due to a strong coupling of the structural and secondary processes, and the experimental dependences τ(T) obtained for secondary relaxations can meet different scenarios, i.e., they can obey the Arrhenius law but often with the values of its parameters, which are different from those valid for the glassy state, or deviate from the Arrhenius equation at all [62].

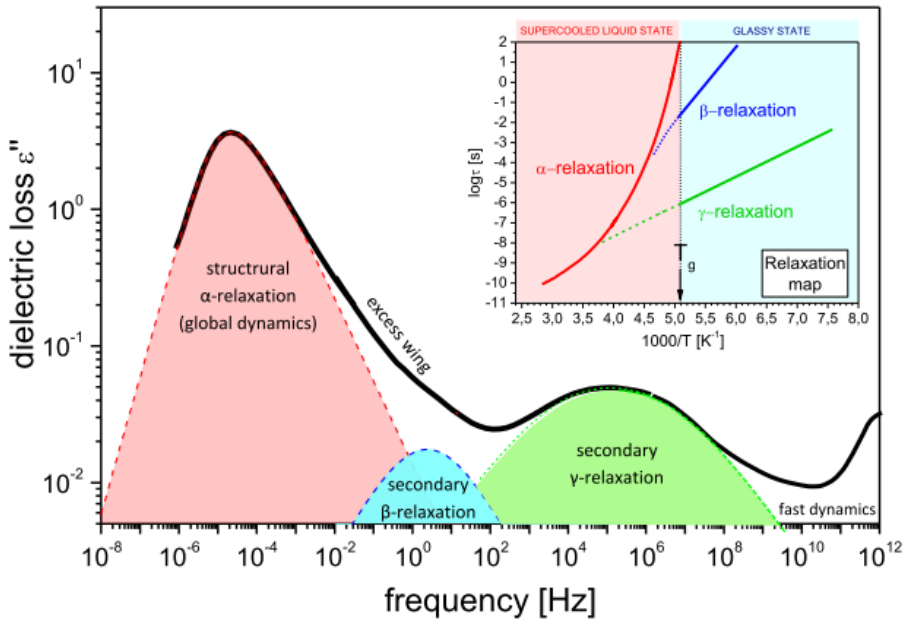

Fig.3 Illustration of dielectric spectra obtained in the broad frequency range after subtraction of the DC conduction contribution and the corresponding relaxation map (inset)

3. Dielectric relaxations in the liquid and glassy states of drugs as physical factors which can govern crystallization

Despite a lot of effort put into studying the effect of the molecular mobility on the physical instability of amorphous drugs, a final adjudication which kind of molecular motions (reflected in structural, secondary or other processes) is responsible for the recrystallization of amorphous APIs still remains an important challenge issued to pharmaceutical sciences. Nevertheless, a progress recently made in this field allows us to believe that we will be able to

enhance the physical stability of amorphous drugs by changing their molecular mobility if we find and understand the molecular mechanisms that govern the recrystallization of amorphous materials. In this Section, we discuss the results that show how the molecular mobility reflected in the structural and secondary relaxation processes as well as the molecular dynamics investigated at THz frequencies can affect the physical instability of amorphous pharmaceuticals and be useful in predicting their tendency to recrystallization.

3.1 Global (structural) α-relaxation

The structural relaxation process, which is responsible for the liquid-glass transition and reflects cooperative and correlated motions of many molecules together, has been also suspected to exert an effect on the recrystallization from the supercooled liquid and glassy states. For instance, some investigations carried out for indomethacin [63,64], celecoxib [11,65], ezetimibe [66], griseofulvin [67], intraconazole,[68] trehalose [69] have suggested that the recrystallization of drugs in the glassy state can be caused by the molecular motions reflected in the structural α-relaxation. Many attempts have been made to correlate some properties of α-relaxation in the supercooled liquid state (such as the fragility parameter, the stretching parameter of nonexponential spectral broadening, and the time and length scales of the structural α-relaxation) with the tendency of drugs to recrystallization from both the supercooled liquid and glassy states as well as with the ability of supercooled liquids to glass formation.

3.1.1 Is there a correlation between the α-relaxation factors determined in the liquid state and the physical stability of disordered solids?

Fragility

The fragility parameter *m* propagated by Angell [70,71] to characterize the sensitivity of molecular dynamics of supercooled liquids to changes in temperature near the glass transition has a few definitions, among which the kinetic definition [72] given below is most commonly acknowledged and reflects the mentioned physical meaning of the parameter in the best way

$$m \equiv \left. \frac{d \log_{10} \tau_\alpha}{d(T_g / T)} \right|_{T=T_g} \qquad (4)$$

It is worth noting that this definition is valid in both isobaric and isochoric conditions [73,74], but the former conditions are usually relevant to pharmaceutical applications, because different measurements are typically carried out at a constant pressure (e.g. at ambient pressure). For isothermal conditions, in which high pressure experiments are often performed, one can define the isothermal fragility parameter [73,74,75] by replacing the temperatures T and T_g respectively with the volumes V and V_g (where the latter is the glass transition volume) in Eq. (4). Recently, some general rules prospected for the fragility parameters defined in different thermodynamic conditions have been formulated [76] and the relative contribution of temperature and density fluctuations to molecular dynamics (possible to evaluate from the ratio of the isochoric and isobaric fragilities [19,18]) have been postulated to play a potential role in the physical instability of amorphous drugs, [41].

In terms of the isobaric fragility parameter, glass-forming liquids can be classified as "strong", "moderately fragile", and "fragile" materials, usually using the following ranges of the value of *m*: $m \leq 30$, $30 < m < 100$, and $m \geq 100$, respectively. The value of the parameter *m* can be regarded as a measure of the sensitivity of molecular mobility to changes in temperature near T_g. The molecular mobility of "fragile" liquids upon approaching the glass transition varies rapidly in contrast to that of "strong" materials. The fragility parameter *m* is closely related to the activation energy for α-relaxation E_a at T_g, $E_a(T_g) = mRT_g \ln(10)$, where the isobaric activation energy is defined [77] as $E_a(T) \equiv Rd \ln \tau_\alpha / d(1/T)$ at a constant pressure and *R* is the gas constant. It means that fragile liquids are characterized by a higher ratio $E_a(T_g)/T_g$ in comparison with strong materials. The steepness index *m* also reflects a degree of the deviation of the dependence $\tau_\alpha(T)$ from the Arrhenius law (Eq. (3)), which is more pronounced for large values of *m*. The fragility has been often regarded as a key factor which can correlate with the glass-forming ability and the physical stability of the amorphous systems, which are both considered to be higher for strong materials [31,78,11,27,24,79,80]. The additional rationale for the special role of the fragility parameter has been provided by Tanaka [81] in his two-order-parameter (TOP) model, which has been successfully demonstrated in simulations [82]. According to this model, a liquid does not crystallize near the glass transition due to some frustrations caused by a locally favored short-range ordering, although the liquid tends to order into an equilibrium crystal characterized by a long-range ordering. The frustrations act as impurities preventing the crystallization, leading to an increase in the free-energy barrier for nucleation. Consequently, they facilitate the vitrification

process. The frustrations of fragile systems against crystallization are weaker than those of strong materials. Therefore, fragile systems should have a weaker glass-forming ability and easier crystallize than strong glass formers (see Fig 4(a)).

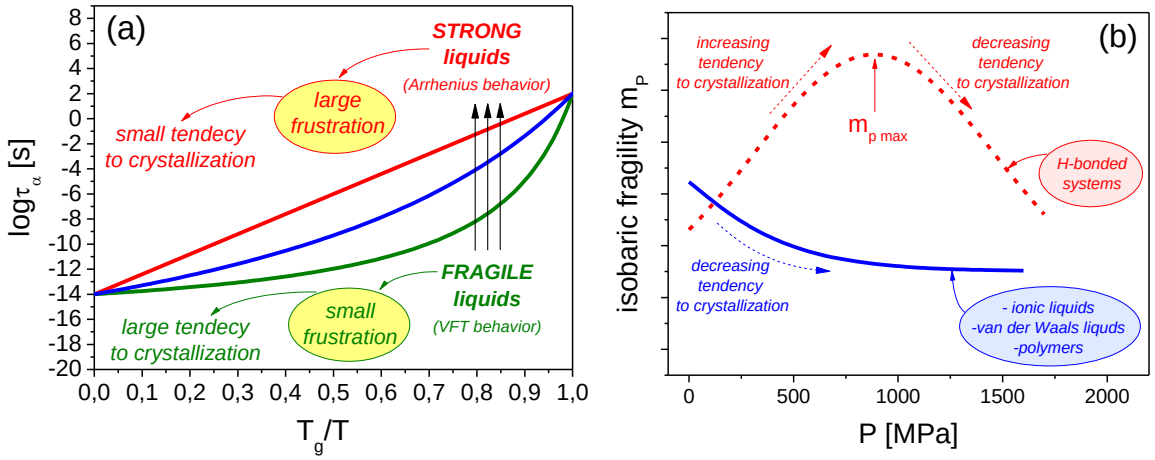

Fig. 4 (**a**) Illustration of the Tanaka concept of frustration against crystallization. The fragile system potentially easier crystallizes because its frustration against crystallization is weaker than that in a strong material. (**b**) Illustration of the typical decreasing pressure dependence of the isobaric fragility *m* and the non-monotonic pressure effect on *m* observed for associated liquids. Both the scenarios potentially reflect differences in the physical stability of systems under compression depending on their ability to forming H bonds.

It is worth noting that the potential correlation of the fragility with the glass-forming ability and the physical stability could be exploited to predict the tendency to recrystallization of amorphous drugs under high pressure (e.g. applied during the tableting process). This is an attractive idea in the context of the recent reports that even a small compression causes the recrystallization of some amorphous drugs such as celecoxib and its solid dispersions [83], ezetimibe,[66], etoricoxib [84], and indomethacin [38]. Previous high pressure BDS studies and some theoretical investigations have shown that the isobaric fragility monotonically decreases with increasing pressure for most material groups (including van der Waals liquids, polymers, and ionic liquids) [73,76,18,19]. It could suggest that the elevated pressure should inhibit the recrystallization of the materials (see Fig 4(b)). An opposite pattern of behavior has been observed only for associated liquids, for which the isobaric fragility usually increases during their compression to some value of pressure and then begin to decrease [85]. This untypical nonmonotonic behavior can be explained by competing effects of densification and increasing temperature on the hydrogen bonding during compression (considered at τ_α=*const*, e.g. along the glass transition line assumed at $\tau_\alpha(T,P)$=100s). An increase in pressure causes a decrease in intermolecular distances, which initially promotes the hydrogen bonding,

however, a continuous increase in temperature associated with the isochronal compression breaks the hydrogen bonds. Nevertheless, the latter effect begins to dominate starting from some sufficiently high value of pressure (the order of 1GPa for oligomers of propylene glycol) and is most probably irrelevant to the drug manufacturing, because the tableting process is carried out at considerably smaller pressures than 1 GPa. The patterns of the pressure behavior of isobaric fragility *m* observed at relatively low elevated pressures could be helpful in assessing the potential risk of recrystallization of amorphous drugs upon the tableting process. Since molecules of many APIs and pharmaceutical excipients strongly interact by hydrogen bonds, the initial increase in the isobaric fragility is expected for these materials under compression. It would suggest that the tableting process could facilitate the recrystallization of the amorphous pharmaceutical solids that are characterized by hydrogen bonds. To test this potentially useful hypothesis, further high pressure studies of pharmaceuticals are required, which have been recently only initiated (see Section 5).

Many attempts have been made to experimentally verify the predicted relationships of the liquid fragility *m* determined at ambient pressure with the glass-forming ability and the physical stability of amorphous materials, including pharmaceuticals [86,87]. Results of the investigations are not unambiguous, and especially the suggested correlation between *m* and the tendency of amorphous drugs to crystallization is questionable [88,87,25]. Although pharmaceuticals mainly belong to fragile and moderately fragile materials, their physical stability can be extremely different. For instance, the isobaric fragilities (established from BDS measurements at ambient pressure) are equal to 98 for etoricoxib and 97 for celecoxib, but amorphous forms of the materials prepared by quench-cooling have different crystallization behaviors (etoricoxib is resistant against the recrystallization at ambient pressure, while celecoxib very easily recrystallizes) [84]. Etoricoxib may exist as a dynamic mixture of two different tautomers, which prevent the API crystallization, while molecules of celecoxib form homodimers by hydrogen bonding, which facilitate a formation of crystal nuclei. These different physicochemical properties are not distinguished by the values of *m*, but determine the tendency of etoricoxib and celecoxib to crystallization. In general, there can be several reasons for the problems observed with the correlation between *m* and the physical stability in case of many different APIs: [23] (i) The single parameter (*m* calculated for a given material at T_g at ambient pressure) can be insufficient to exhaustively reflect a lot of interplaying properties of APIs such as specific interactions (hydrogen bonding or ionic interactions), various molecular structures, flexibility and conformational changes of molecules, formation of special intermolecular structures like dimers, and chemical reactions

like tautomerization, which can occur near the glass transition as well as in thermodynamic conditions at which amorphous drugs are stored or manufactured. (ii) Based on the classical theory of crystallization [89], the overall crystallization is consisted of the processes of nucleation and crystal growth, which involve both thermodynamic and kinetic contributions that vary with changing thermodynamic conditions (T and P) (see Section 5). Moreover, applied amorphization methods, storage or manufacturing humidity as well as impurities, defects, and mechanical tensions in examined samples can influence the tendency to crystallization. Thus, the single fragility parameter may be unable to predict the possible variety of crystallization events. (iii) In addition, a determination of reliable values of *m* often causes difficulties, which can result even in misleading conclusions.

The latter point is worthy of detailed considerations. Although there are different thermal methods for predicting the fragility parameter [90,86,25,87], we would like to stress that a reference for all the predictions should be the dynamic fragility directly determined from global molecular mobility studies according to the definition given by Eq. (4) which in the best way reflects the physical meaning of this parameter (that is a measure of the sensitivity of molecular dynamics of supercooled liquids to changes in temperature near the glass transition). We share the opinion expressed by Johari et al. [91] that BDS and viscosity measurements (as well as other measurements of relaxation processes) provide experimental data that enable us to find the accurate temperature dependences $\tau_\alpha(T)$ in the sufficiently wide temperature range near T_g, which consequently allow to determine the most reliable values of the parameter *m* defined by Eq. (4). To do that one should well describe the experimental dependence $\tau_\alpha(T)$. This goal is usually satisfactorily achieved (e.g. for sildenafil dielectric data in Fig. 5(a)) by the commonly used VFT equation (Eq. (2)), the parameters of which enable to calculate the value of the fragility $m = D(T_0/T_g)\Big/\left[(1-(T_0/T_g))^2 \ln(10)\right]$. However, one should remember that the dependence $\tau_\alpha(T)$ in case of many glass forming liquids cannot be well fitted to a single VFT equation and two VFT functions have to be applied to describe such data (e.g. for ibuprofen, telmisartan, salol, glycerol [92,93,42,94] or ezetimibe [66] shown in Fig. 5(b)). Stickel [95] proposed a useful method for distinguishing these two temperature regions for the VFT equations obeyed with different values of their parameters. This method is based on a differential operator $\left[d\log_{10}\tau_\alpha / d(1/T)\right]^{-1/2}$, which linearizes the VFT formula and enables to establish one or two linear regions for the temperature dependences of this operator. The dynamic crossover at the crossover temperature T_{cross} and the corresponding crossover structural relaxation time τ_{cross} at which the change occurs in the

VFT equations is usually interpreted as a reflection of substantial change in the molecular mobility responsible for the structural relaxation, which most probably have a strongly cooperative character only at $T<T_{cross}$ and $\tau_\alpha>\tau_{cross}$. As can be seen for ezetimibe, the crossover time scale τ_{cross} can be relatively high (i.e., considerably larger than $\tau_\alpha=10^{-6}$s above which the cooperative dynamics is often arbitrarily assumed), therefore, a good practice is to apply the Stickel method to support the analysis of the dependence $\tau_\alpha(T)$ by using the VFT equation.

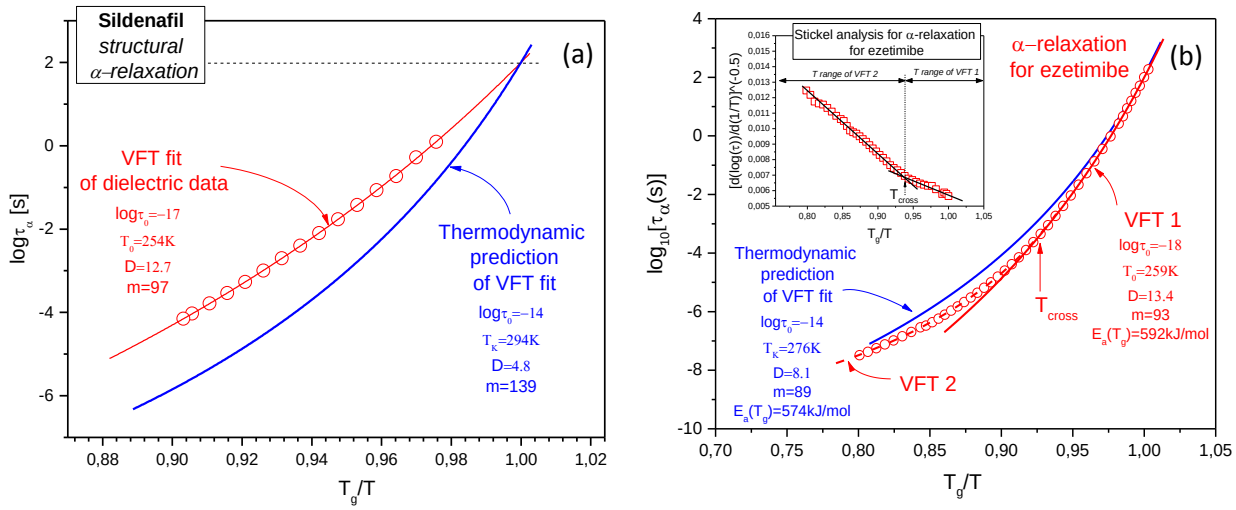

Fig. 5 (**a**) Illustration of a significant difference in the values of the isobaric fragility (defined by Eq. (4)) found from thermodynamically evaluated parameters of the VFT equation (Eq. (2)) and determined directly from experimental dielectric data also by applying Eq. (2) in case of sildenafil (dielectric data taken from Ref. [100]). (**b**) An analogous comparison for ezetimibe (dielectric data taken from Ref. [66]) additionally demonstrates that two VFT equations are required to properly describe some temperature dependences of structural relaxation times, and consequently reliably determine the fragility parameter. The inset in panel (b) shows how to identify the separate fitting regions to Eq. (2) according to Stickel's approach.

Some problems with evaluating proper values of *m* also result from the applied prediction methods. One of the most popular approaches to evaluate the dynamic fragility parameter m for various pharmaceutical systems is to estimate the VFT equation parameters by using calorimetric measurements. Based on the assumptions that (i) the VFT divergence temperature T_0 is equal to the Kauzmann temperature T_K, which can be estimated from different thermodynamic relations [24,88,90], (ii) the preexponential factor representing the time scale of vibrational motions $\tau_0=10^{-14}$s, and (iii) the structural relaxation time $\tau_\alpha=100$s at T_g, one can calculate the strength parameter $D=16\ln(10)(T_g-T_K)/T_K$ and

$m = D(T_K/T_g)/\left[(1-(T_K/T_g))^2 \ln(10)\right]$ from the VFT equation (Eq. 2). It should be noted that this prediction method can yield misleading results, because its assumptions may not be met. For example, for ezetimibe and sildenafil, the values of the parameters τ_0, T_0 and D obtained from fitting the experimental dependences $\tau_\alpha(T)$ to Eq. (2) clearly differ from the assumed τ_0=$10^{-14}s$ and the values of T_K and D estimated from thermodynamic data (using $T_K^{-1} = T_m^{-1}(1+\Delta H_m/C_{Pconf}T_g)$ [90]). Discrepancies between experimental and predicted temperature dependences of τ_α and fragilities *m* can be well demonstrated as a function of the ratio T_g/T in the so called Angell plot (see Fig. 5). In case of sildenafil, a large difference is found between the predicted value m=139 and the value m=97 obtained from $\tau_\alpha(T)$ determined from experimental dielectric data. For ezetimibe, the predicted value m=89 is in accord with the value m=93 obtained from the experimental dependence $\tau_\alpha(T)$. Nevertheless, the case of ezetimibe shows the parameter D in Eq. (2), which is often alternatively considered as a measure of fragility, can be improperly predicted from thermodynamic data even if the parameter *m* is well estimated.

Non-exponentiality of dielectric α-relaxation response - β_{KWW}

The next factor potentially responsible for the physical instability of amorphous pharmaceuticals is the asymmetric distribution of molecular relaxation times, which is a characteristic of structural relaxation process [30,91,96,97,9,11,66]. A commonly used measure of the α-relaxation time distribution is the stretching parameter β_{KWW} of the Kohlraush-Williams-Watts (KWW) function [98]

$$\phi(t) = \exp\left[-\left(\frac{t}{\tau_{KWW}}\right)^{\beta_{KWW}}\right], \qquad (5)$$

where τ_{KWW} is the characteristic KWW relaxation time and the parameter $0<\beta_{KWW}\leq 1$ quantifies the deviation of the time-dependent relaxation function from the Debye exponential decay (for which β_{KWW}=1). The dielectric spectra obtained in the frequency domain from the BDS measurements can be described by the KWW function after its numerical Fourier transformation to the frequency domain. The nonexponentiality of the dielectric response function for non-Debye relaxations can be explained by assuming some distribution of molecular relaxation times (which means that molecules in the sample reorient with different relaxation times) instead of the same relaxation time for each molecule in given thermodynamic conditions in the case of Debye relaxation. Shamblin et al. [30] suggested that

the distribution of structural relaxation time may raise the crystal nucleation rate, and consequently the "shelf life" of a pharmaceutical can be correlated with β_{KWW}. Based on investigations of different statistical distributions, the authors reported that both the physical and chemical stability should decrease when β_{KWW} decreases (i.e., when the distribution of structural relaxation time broadens). It has been also pointed out that faster modes of molecular motions within the distribution of relaxation times can be responsible for nucleation in the glassy state, therefore, the glass formers characterized by small values of β_{KWW} would be more susceptible to nucleation [99]. However, it should be emphasized that the expected correlation between β_{KWW} and the tendency to crystallization is not met by all pharmaceuticals. For example, celecoxib [11], sildenafil [100], ezetimibe [66], and acetaminophen [91] have narrow structural relaxation dielectric spectra near the glass transition (characterized by large values of β_{KWW} = 0.67, 0.68, 0.70, and 0.79 respectively), while the drugs easily recrystallize from their amorphous forms.

The stretching parameter β_{KWW} has been often considered as a measure of the degree of cooperativity and the length scale or dynamic heterogeneity of molecular mobility reflected in the structural relaxation [72,101]. Thus, β_{KWW} has been also regarded as the alternative parameter to the fragility index *m* in search of correlations with the tendency to crystallization, which are aimed at predicting the physical stability of amorphous pharmaceuticals. A large interest aroused an empirical linear correlation suggested by Böhmer et al. [72] between the fragility *m* and the parameter β_{KWW}, m=250±30-320β_{KWW}. According to this correlation, fragile materials (large *m*) should be characterized by broad structural relaxation peaks near T_g, i.e., a high nonexponentiality of dielectric relaxation response (small β_{KWW}). On the other hand, strong glass formers (small *m*) should exhibit narrow relaxation peaks, i.e., a low nonexponentiality of dielectric relaxation response (large β_{KWW}) near T_g. It should be noted that the suggested effect of the distribution of molecular relaxation times on the crystal nucleation rate well complies with the Böhmer correlation, i.e., the small fragility *m* and large β_{KWW} should imply a weak tendency to crystallization (see Fig. 6). However, there are known examples of materials, including drugs, which do not satisfy the correlation suggested by Böhmer *et al*. Among such pharmaceuticals, one can expect that at least one of the potential physical instability factors, *m* or β_{KWW} misleadingly predicts the tendency to recrystallization of amorphous forms of the drugs (as it is in the case of celecoxib, sildenafil, ezetimibe, and acetaminophen, which are characterized by relatively large values of *m* and β_{KWW}).

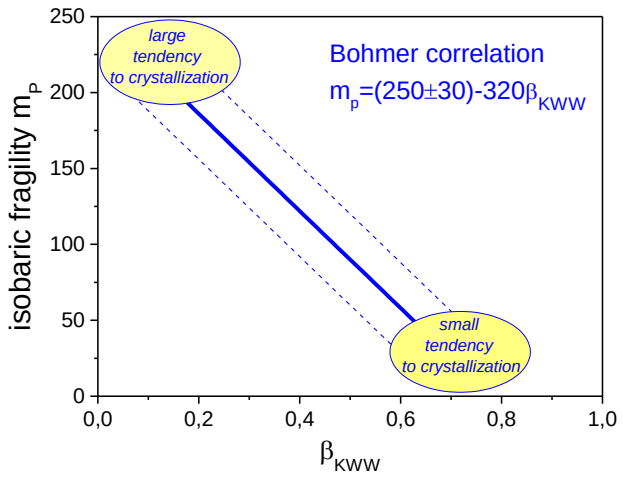

Fig. 6 Illustration of the correlation suggested by Böhmer *et al*. between the isobaric fragility and the stretching parameter of the KWW function as well as its potential implications for the tendency to crystallization.

In addition, it is worth noting that also the pressure behavior of β_{KWW} does not correlate with the pressure effect on *m* for many materials. When the isobaric fragility typically decreases with increasing pressure (with the exception of associated liquids), the stretching parameter β_{KWW} usually remains unchanged (especially in isochronal conditions at τ_α=*const*) [102], whereas the compression often affects the physical stability of amorphous drugs.

Dynamic heterogeneity

The physical meaning of the parameters *m* and β_{KWW} has been potentially related to both the fundamental characteristics which are often assumed for molecular dynamics near the glass transition, which are its cooperativity and dynamic heterogeneity. Since a potentially important role of the dynamic heterogeneities of molecular dynamics in the formation of crystal nuclei has been recently argued by theoretical and simulation investigations [103,104,105,106,107,108], the search for the proper measure of the dynamic heterogeneity and the studies of the potential correlation of the dynamic heterogeneity with the physical instability of amorphous drugs constitute a highly promising research trend nowadays. There are different measures of the characteristic size of the dynamic heterogeneity [109]. In the last decade, the formalism of the four-point dynamic correlation function has been successfully developed to quantify the spatially heterogeneous dynamics near T_g due to involving both temporal and spatial correlations [110,111]. The height of the peak χ_4^{max} of the four-point time dependent dynamic susceptibility function $\chi_4(t)$ has been acknowledged as a good measure of the dynamic heterogeneity, which should be mainly interpreted as the correlation

volume for the structural relaxation, but it is also approximately considered as an average number of dynamically correlated molecules. Since direct experimental measurements of $\chi_4(t)$ are complex, because they require detecting nonlinear response of the sample, Berthier *et al.* [110,111] suggested a few estimates of $\chi_4^{\max}$ derived by using the fluctuation-dissipation theorem. The estimate convenient to use is based on enthalpy fluctuations, which involves both temperature and density fluctuations that affect the molecular mobility,

$$\chi_4^{\max} \approx \frac{R}{\Delta c_p}\left(\frac{\beta_{KWW}}{e}\frac{d\ln\tau_\alpha}{d\ln T}\right)^2 \qquad (6)$$

where Δc_p is the difference in the isobaric heat capacities between the liquid and glassy states. It is worth noting that Eq. (6) enables to evaluate values of $\chi_4^{\max}$ at different temperatures in isobaric conditions by using calorimetric and dielectric data. Interestingly, it has been established [110,112] that $\chi_4^{\max}$ correlates with neither *m* nor β_{KWW} for different materials at ambient pressure. In addition, analyses of high pressure experimental data have shown that the pressure induced changes in the dynamic heterogeneities quantified by the estimates of $\chi_4^{\max}$ at $\tau_\alpha = const$ do not cause any variations in β_{KWW} for each examined material (including also a pharmaceutical material glibenclamide) [113]. These findings suggest that neither *m* nor β_{KWW} properly reflect the dynamic heterogeneity or the dynamic length scale $\xi_4^{\max}$ of molecular dynamics, which results from the correlation volume $\chi_4^{\max}$ (in the simplest way via the relation, $\chi_4^{\max} \approx \left(\xi_4^{\max}/a\right)^{\psi}$, where ψ=3 and the molecular size $a = \upsilon_m^{1/3}$ for the molecular volume υ_m). A successful attempt has been made [100] to correlate $\chi_4^{\max}$ evaluated from Eq. (6) by using the temperature dependence of the dielectric structural relaxation times with both the induction time of nucleation and the characteristic overall crystallization time for sildenafil in isothermal conditions above T_g. As a result, it has been shown that the increase in the dynamic heterogeneity causes a slowdown in diffusion, and consequently the crystallization of sildenafil becomes slower.

It should be noted that there is another useful measure that can be a good alternative to the estimate of $\chi_4^{\max}$ based on enthalpy fluctuations. This alternative approach, which exploits heat capacity measurements, has been formulated by Donth,[114,115] who also relied on the fluctuation-dissipation theorem but considered entropy fluctuations at the glass transition. Although Donth originally elaborated his method to evaluate a size of the cooperatively rearrangement regions (CRR) postulated by Adam-Gibbs theory, the formulation way and the

quantitative results yielded by the Donth estimate show that this method should be rather classified as a measure of the dynamic heterogeneity than the cooperativity of global molecular mobility near T_g [111,116]. Vyazovkin and Dranca [117] compared the dynamic length scale ξ=3.4nm determined for indomethacin from the Donth method with the critical size of crystallization nucleus r^* that ranges from 0.7 to 0.9 nm depending on polymorphic crystalline forms of the drug. As a result, the authors stated that a critical nucleus could be formed even without involving cooperative motions related to the structural relaxation, because r^* is considerably less than the length scale ξ of the global molecular mobility in indomethacin. Consequently, the formation of the critical nuclei have been suggested to occur in indomethacin only via the local noncooperative motions of the individual molecules (e.g. those reflected in the JG secondary process) at least in the temperature region of the secondary β-relaxation. Using the Donth method, Kawakami [118] investigated the length scale ξ of ribavirin during an annealing of the drug, finding that an enhancement of the crystallization rate below T_g may be correlated with an increase in ξ.

There is currently a need for such analyses based for instance on Donth or Berthier methods, which enable to evaluate the dynamic length scale or the correlation volume for the structural relaxation, to gain a better insight into potential correlations of fundamental parameters of molecular dynamics with the tendency to recrystallization. Especially that until now, mainly time scales of different relaxation processes have been investigated in search of correlations with characteristic crystallization rates (see Section 3.1.2.2), while also the length scale of molecular dynamics may affect the recrystallization process in both the supercooled liquid and glassy states.

3.1.2 Time scales of crystallization and structural relaxation in the liquid and glassy states

Amorphous pharmaceuticals reveal different tendencies to recrystallization. Some of them are very good glass formers and in general they are resistant to recrystallization, the other ones recrystallize from the supercooled liquid state but their glassy forms are physically stable during their storage, and the others easily recrystallize both in the glassy and liquid states. To gain a better insight into understanding of nucleation and crystal growth mechanisms, a lot of effort has been put into combined studies of the crystallization phenomena of the amorphous pharmaceuticals near their glass transition and different kinds

of molecular mobility that can be responsible for the recrystallization from both the supercooled liquid and glassy states. A particular emphasis has been laid to compare or/and correlate characteristic time scales of crystallization (such as the induction time for nucleation t_0 and the overall crystallization rate τ_{cr}) with relaxation times of the structural process as well as the secondary relaxation processes. To determine the characteristic parameters of nucleation and crystal growth, experiments of crystallization kinetics are performed by using different techniques (calorimetric, X-ray diffraction, and microscopic ones) [69,119,120,121,122,123,124], including the dielectric spectroscopy that is a powerful method for detecting the recrystallization of drugs and quantifying its kinetics at both ambient and elevated pressures [125] (see Section 5). While the crystallization rates can be experimentally established both in the supercooled liquid and glassy states, the structural relaxation times are extremely large in the glassy state, and their measurements are highly time consuming. It should be emphasized that the glassy dynamics is especially important for the physical stability studies of amorphous pharmaceutical solids, which are stored at $T<T_g$, and both the global and local relaxation processes can be responsible for the recrystallization of glassy drugs. In such studies, to consider the molecular mobility reflected in the structural relaxation below T_g, a few methods have been proposed to predict the time scale of α-relaxation at $T<T_g$, which are outlined before the discussion on the correlations between crystallization and relaxation time scales of pharmaceutical materials.

3.1.2.1 Predictions of the temperature dependence of structural relaxation times in the glassy state

Prediction of $\tau_\alpha(T)$ in the glassy state by a master plot construction

One of the simplest methods for determining the structural relaxation times in the glassy state consists in the construction of a master plot[11,66,9] by horizontally shifting a selected structural relaxation loss peak (for which both low and high frequency flanks are well measured in the liquid state in the close vicinity of T_g) to lower frequencies in order to overlap loss spectra collected at lower temperatures ($T<T_g$) for which only high frequency flanks of the α-loss peak are experimentally well determined (see Fig. 7). Then, from the frequencies at which the maxima of the shifted α-peak occur at different temperatures below T_g, the structural relaxation times can be evaluated at $T<T_g$. Such an evaluation procedure of the α-peak positions below T_g is permitted only if the shape of structural relaxation peak is

almost temperature independent. It is considered that the master plot construction yields reliable values of τ_α in the glassy state at temperatures sufficiently close to T_g, at which the evolution of the glassy system towards an equilibrium is fast. At temperatures well below T_g, the glass slower evolves to an equilibrium, and then the values of τ_α predicted by constructing the master plot may deviate from the proper time scale of structural relaxation.

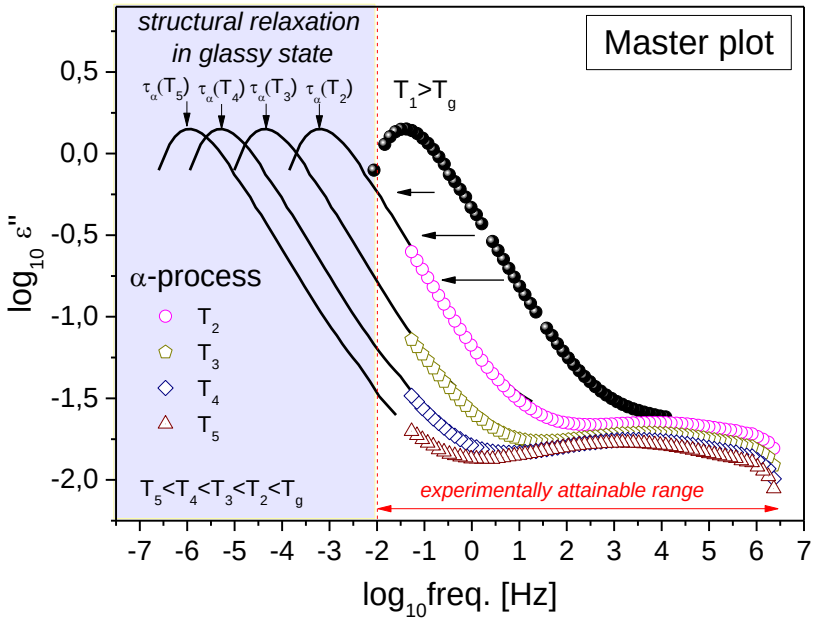

Fig. 7 Illustration of the master plot constructed by horizontally shifting the loss peak measured at $T_1>T_g$ to overlap spectra at T_5, T_4, T_3, T_2 obtained below T_g

Predictions of $\tau_\alpha(T)$ in the glass state by the extended Adam-Gibbs model

A commonly used method for evaluating τ_α below T_g is based on the Adam and Gibbs (AG) model [61] extended [29,126,31] into the glassy state. According to the extended AG approach, the temperature dependence of structural relaxation times can be predicted from the following formula

$$\tau_\alpha\left(T,T_f\right)=\tau_0\exp\left(\frac{DT_0}{T\left(1-T_0/T_f\right)}\right), \qquad (7)$$

where τ_0, D, T_0 are the fitting parameters found from the VFT equation (Eq. 2) for the dependence $\tau_\alpha(T)$ in the liquid state. The fictive temperature T_f in Eq. 7 depends on temperature, $T_f^{-1}=\gamma_{Cp}T_g^{-1}+(1-\gamma_{Cp})T^{-1}$, and can vary between the Kauzmann temperature T_K and the glass transition temperature T_g. The value of T_f can be estimated by using a thermodynamic parameter γ_{Cp} defined by the heat capacities of liquid, glass, and crystal at T_g

as follows $\gamma_{Cp} = \left(C_p^{liq}(T_g) - C_p^{gl}(T_g)\right) / \left(C_p^{liq}(T_g) - C_p^{cryst}(T_g)\right)$. If $\gamma_{Cp} = 1$ then T_f =T_g and Eq. (7) represents the Arrhenius law. On the other hand, Eq. (7) becomes the standard VFT equation if $\gamma_{Cp} = 0$ for which T_f =T. This useful approach, which is capable to describe the molecular dynamics between the strong and fragile behavior patterns (i.e., between Arrhenius and VFT dependences), cannot be however satisfactorily employed in the case of pharmaceuticals for which we cannot reliably establish experimentally the heat capacity of their crystal phase (e.g. for crystalline hydrates often found among drugs and some polymers used as excipients that are not prone to crystallization).

Predictions of $\tau_\alpha(T)$ in the glassy state by the extended Avramov model

Difficulties in determining the temperature dependences of the heat capacity in the crystal state for some materials, can be avoided by using the extended Avramov model to predict the dependence $\tau_\alpha(T)$ in the glassy state. Adam and Gibbs originally assumed that the thermodynamic evolution of the time scale of structural relaxation depends on the product of temperature T and configurational entropy S_{conf}, $\log_{10}\tau_\alpha = \log_{10}\tau_0 + C_{AG}/TS_{conf}$, where τ_0 and C_{Av} are fitting parameters. In the physical stability studies of amorphous drugs, the configurational entropy is considered as an excess entropy of disordered states (liquid and glass) with respect to the crystal entropy $S_{conf} = S^{disorder} - S^{cryst}$. In contrast to the AG approach, Avramov postulated that thermodynamically induced changes in structural relaxation times can be described by a function of the total system entropy S, $\log_{10}\tau_\alpha = \log_{10}\tau_0 + C_{Av}\exp\left[-B_{Av}\left(S - S_r\right)\right]$, where τ_0, C_{Av}, and B_{Av} are fitting parameters and S_r is the total system entropy determined at a chosen reference state (e.g. at T_g at ambient pressure). Although high pressure analyses have shown that the original Avramov model requires some modifications [127,128], it has been very recently suggested that the original form of the Avramov model is sufficient to predict $\tau_\alpha(T)$ below T_g to a good approximation [129]. The simple prediction procedure is based on the measured temperature dependences of the isobaric heat capacity $C_p(T)$ near the glass transition in the liquid and glassy states and the structural relaxation times $\tau_\alpha(T)$ at T>T_g. By exploiting the experimental data $C_p(T)$, one can find the temperature dependence S(T) above and below T_g (based on the known equation $S(T) = S_r + \int_{T_r}^{T} C_p(T) d\ln T$). It means that the extended Avramov approach relies only on $S^{disorder}$ that is the entropy of disordered states (liquid and glass). By fitting the dependence τ_α(S)

above T_g to the Avramov entropy dependent model, one can determine the values of its parameters τ_0, C_{Av}, and B_{Av}, which are subsequently used to generate the structural relaxation times τ_α below T_g from this model as a function of S or T, employing the dependence S(T) established from calorimetric data below T_g and brought into the extrapolated equilibrium line. As can be seen in Fig. 8 , in case of carvedilol, all the prediction methods discussed before, i.e., the master plot construction as well as the extended Adam-Gibbs and Avramov models yield consistent results.

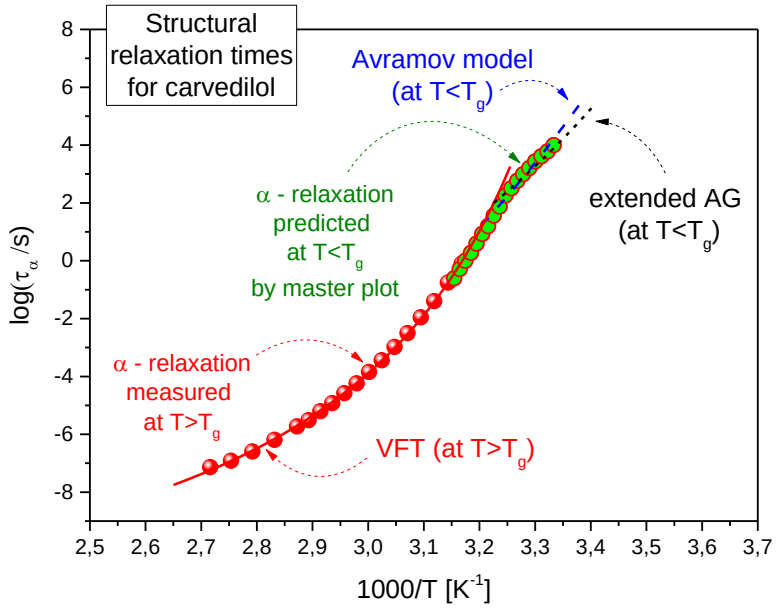

Fig. 8 Example of consistent predictions of structural relaxation times below T_g by constructing the master plot (green circles with red edge) and by using the extended AG and Avramov models (short dashed and dashed curves, respectively) for carvedilol (data taken from Ref. [129])

Predictions of $\tau_\alpha(T)$ in the glassy state by using the extended coupling model for the JG secondary relaxation

Since the JG secondary relaxation is considered as a precursor of the structural relaxation and a correlation between the JG- and α-relaxations has been reported,[130,131] some methods for predicting $\tau_\alpha(T)$ at $T<T_g$ refer to this intermolecular secondary process. One of the approaches assumes that the separation in time between the structural and JG secondary processes is of the same order as the separation between τ_α and the primitive relaxation time τ_p of the coupling model (CM) model (i.e., the JG secondary relaxation time $\tau_{JG} \approx \tau_p$). According to the extended CM formulated to identify the JG process,[132] (see Section 3.2), the JG secondary relaxation time, $\tau_{JG} \approx t_c^{1-\beta_{KWW}} \tau_\alpha^{\beta_{KWW}}$, where t_c=2ps for small molecular and

polymeric glass formers. Thus, one can predict the temperature dependence of the structural relaxation times τ_α in the glassy state from the equation, $\log_{10}\tau_\alpha(T) = \beta_{KWW}^{-1}\log_{10}\tau_{JG}(T) + \beta_{KWW}^{-1}(\beta_{KWW}-1)\log t_c$, by exploiting β_{KWW} established for the experimental loss peak of structural relaxation in the liquid state near T_g as well as the dependence $\tau_{JG}(T)$ determined from the loss spectra measured below T_g for the secondary relaxation classified as the JG process. It is worth noting that this prediction model implies that the ratio of the activation energy for structural and JG secondary relaxations depends on the asymmetric broadening of the structural relaxation loss peak near T_g as follows $E_a^\alpha = \beta_{KWW}^{-1}E_a^\beta$.

Predictions of $\tau_\alpha(T)$ in the glassy state by using physical aging of the secondary relaxation

Since the glassy state is thermodynamically non-equilibrium, physical properties of a glass depend on the thermodynamic path and change during the physical aging, i.e., the slow evolution of the glass toward equilibrium. Casalini and Roland [133] (CR) demonstrated that the changes in the JG secondary relaxation during the physical aging of glass also give information about a very slow structural relaxation in the glassy state. Upon aging the α-peak moves to lower frequencies and its contribution to the β-process is smaller, whereas the position β-peak remains unchanged but the amplitude of the β-relaxation decreases. This behavior seems to be caused by a decrease in the population of relaxing dipoles due to decreasing local density fluctuations during the physical aging. Thus, such changes in the β-relaxation likely probe structural relaxation dynamics unattainable experimentally in the glassy state. Analyzing isothermal time-dependent measurements of the imaginary part of the dielectric permittivity *ε"*(*f*) during the physical aging at a few fixed frequencies *f* (in the range of β-relaxation peak) by using an empirical time-dependent decay model of the KWW function type, the authors showed that the time scale of the physical aging τ_{ag} depends on temperature but is independent of the frequency at which the changes in the amplitude of β-loss peak have been examined at a given temperature. Casalini and Roland suggested that the aging time scale is determined by the structural relaxation, therefore $\tau_{ag} \approx \tau_\alpha$. Thus, the time scale of α relaxation in the glassy state can be evaluated as τ_{ag} determined from the changes in the β relaxation measured in the physical aging experiments. Interestingly, analogous results can be obtained from the analyses of the physical aging of the non-JG secondary

relaxation [134]. The similar aging time scales obtained for the JG and non-JG secondary processes suggest that the evolution of the glass towards equilibrium can identically affect the intermolecular and intramolecular local mobility in the glassy state (e.g., via decreasing local density fluctuations during the physical aging). Thus, the physical aging experiments carried out on different kinds of secondary relaxations can be useful in predicting the time scale of structural relaxation in the glassy state [135].

3.1.2.2 Correlations between time scales of crystallization and structural relaxation

According to the classical crystallization theory [136], the fundamental time scales of crystallization such as the nucleation rate, the crystal growth rate, and the non-steady-state time lag are affected by thermodynamic and kinetic contributions. In general, it is considered that the kinetically governed part of a crystallization rate depends on the molecular diffusion. Invoking the Stokes-Einstein (SE) equation and the Debye-Stokes-Einstein (DSE) equation, both the translational D_{trans} and rotational D_{rot} diffusion coefficients should be proportional to the ratio of temperature T over viscosity η. In this way, the kinetic contributions to the crystallization rates could inversely depend on viscosity at a given temperature. However, the proportionalities, $D_{trans} \sim T\eta^{-1}$ and $D_{rot} \sim T\eta^{-1}$, which are well satisfied by weakly supercooled liquids, are often broken in the deep supercooled region close to T_g (at $T<1.3T_g$), where decoupling phenomena are observed between diffusion coefficients and viscosity. In these cases, the fractional SE and DSE equations are satisfied, which imply the generalized proportionalities, $D_{trans} \sim T\eta^{-\xi_{trans}}$ and $D_{rot} \sim T\eta^{-\xi_{rot}}$, where the measures of the decoupling phenomena ξ_{trans} and ξ_{rot} vary between 0 and 1 and can be in general different ($\xi_{trans} \neq \xi_{rot}$), which means that a decoupling can be also observed between translational and rotational diffusions [137,138,139,140,141,142]. Analogous fractional equations are also considered for relaxation times τ making an assumption that $\tau \sim \eta$, where the latter proportionality relies on the Maxwell relation between average shear relaxation time and viscosity, $\tau = \eta / G_\infty$, which involves the high-frequency shear modulus G_∞ that is only moderately temperature dependent (usually increasing less than a factor of 4 upon cooling in the temperature range, where τ increases by 10 orders of magnitude [143]). Ediger *et al.* [78] have shown that the kinetic contribution dominates over the thermodynamic contribution to the crystallization growth near T_g and is satisfactorily proportional to $\eta^{-\xi_{trans}}$, where the latter finding obtained by comparing self-diffusion coefficients and viscosities complies [138] with the fractional SE

relation (at *T=const*). It means that there is a decoupling between crystallization rate and viscosity, which can be quantified by the exponent ξ_{trans}. If ξ_{trans}=1, the crystallization rate is coupled with viscosity, and consequently the crystallization process is fully controlled by the translational diffusion, whereas the smaller value of ξ_{trans}, the smaller influence of translational motions on the crystallization process. By analogy, one can investigate the effect of rotational motions reflected in dielectric relaxation processes on the crystallization process. It should be noted that the dielectric spectroscopy can measure only the rotational mobility although both translational and rotational motions contribute to molecular dynamics of supercooled liquids. It means that a translational motion of a molecule without its rotation does not appear in the dielectric relaxation.[99]. Consequently, the correlations established between the crystallization rates and the dielectric relaxation times enable us to study how the crystallization process depends on the rotational diffusion (via the fractional DSE equation for a rotational relaxation time $D_{rot} \sim T\tau_{rot}^{-\xi_{rot}}$, where τ_{rot} can be relaxation times of structural and secondary dielectric processes). Considering the structural dielectric relaxation times τ_α in this context, one should remember that a decoupling phenomenon can be also observed between η and τ_α, which can lead to different values of ξ_{rot} evaluated based on the fractional DSE equations for η and τ_α. Investigations of the potential effect of rotational diffusion on the crystallization process are important, because it seems reasonable to assume that the rotational diffusion rather than the translational diffusion can favor the formation of crystal nuclei between the nearest neighboring molecules [144].

In recent studies, potential relationships between the crystallization rate k (or the characteristic crystallization time $\tau_{cryst} = k^{-1}$) defined in a few ways and different kinds of molecular mobility have been tested by using some linear correlations that can be generalized to the following form,

$$\log \tau_{cryst} = \xi_X \log_{10} X + B \qquad (8)$$

where are two fitting parameters, B and the so-called coupling coefficient ξ_X, which is regarded as is a measure of the coupling between the crystallization phenomenon characterized by τ_{cryst} and the molecular motions probed by a measurement quantity X such as structural and secondary relaxation times, viscosities, and diffusivities. If ξ_X=1, the investigated molecular mobility is assumed to be responsible for the crystallization phenomenon, whereas the smaller value of ξ_X, the smaller effect on the crystallization process is expected due to the examined molecular motions. It is worth noting that the coupling coefficient ξ_X reflects the ratio of the activation energies for the crystallization process

characterized by the time scale τ_{cryst} and the molecular relaxations or other dynamic processes examined via the measurement quantity X, i.e., $\xi_X = E_a^X / E_a^{cryst}$. It means that the molecular relaxations or other dynamic phenomena (e.g. the translational diffusion) rather should not trigger the crystallization process if their activation energies are significantly larger than E_a^{cryst}. In a few cases, the considerably large values ξ_X>1 have been reported, which could not be explained by experimental errors, and then no link has been suggested between the considered molecular mobility and the crystallization process. A collection of results obtained from several investigations based on Eq. (8) is presented in Table 1. The literature data show that the potential influence of the molecular mobility reflected in the structural relaxation on the crystallization time scales defined in a few manners (such as the inverse overall crystallization rate τ_{cr}, the crystallization onset time t_0, the crystal growth rate, and the characteristic crystallization time obtained for 0.5% or 10% degree of crystallization $t_{c(0.5\%)}$ and $t_{c(10\%)}$) has been mainly examined in terms of Eq. (8). Depending on the correlated values, different values of the coupling coefficient ξ_X have been found. For instance, in case of indomethacin, it has been found that the global mobility reflected in α-relaxation above T_g exerts a significantly larger effect on the crystallization onset time ($\xi_{\tau_\alpha} = 0.85$) than that on the crystal growth rate ($\xi_{\tau_\alpha} = 0.29$). This observation suggests that diffusional processes in liquid indomethacin are more involved in controlling the crystal growth than in controlling crystal nucleation, and factors other than diffusion are more important in the nucleation than in the crystal growth [63]. On the other hand, considering $t_{c(10\%)}$ for nifedipine also above T_g, the different coupling coefficients have been determined for the dielectric structural relaxation time $\xi_{\tau_\alpha} = 0.62$ and the translational diffusion $\xi_{D_{trans}} = 0.82$, which mean that the physical stability of liquid nifedipine may be better coupled to translational rather than to rotational motions [13]. The strong influence of the cooperative α-relaxation on the physical stability has been established for intraconazole [68], indomethacin [63], trehalose [69], celecoxib [11], nifedipine-(5%)PVP and nifedipine-(10%)PVP dispersions [145] above T_g as well as for griseofulvin [13], nifedipine [13], and nifedipine-(2.5%)PVP dispersion [13] below T_g. Due to limitations in exploring the structural relaxation and the crystallization kinetics at $T<T_g$, the correlation studies have been usually conducted above T_g, and then their results have been extrapolated to temperatures below T_g. Satisfactorily predictions of the crystallization onset time t_0 below T_g on the basis of its correlations with the structural relaxation time τ_α above T_g have been reported for trehalose [69], indomethacin [63], flopropione [63]. Nevertheless, such

predictions should be carefully used, because it has been shown that the experimental values of the coupling coefficient ξ_{τ_α} determined for the same type of the crystallization time scale may considerably differ in the liquid and glassy states (e.g., for τ_{cr} of griseofulvin,[67] $\xi_{\tau_\alpha} = 0.56$ in liquid and 0.19 in glass, whereas for $t_{c(10\%)}$ of nifedipine, [13] $\xi_{\tau_\alpha} = 0.65$ in liquid and 0.94 in glass). In these cases, a change in the crystallization mechanism likely occurs when the glass transition temperature is crossed. For these drugs, Kothari et al. [13] have also tested the coupling coefficients between $t_{c(10\%)}$ and the secondary β-relaxation times, finding surprisingly large values $\xi_{\tau_\beta} = 2.6$ for griseofulvin and $\xi_{\tau_\beta} = 1.8$ for nifedipine, which indicate that there is no link between the secondary relaxation and the recrystallization of glassy forms of the pharmaceuticals. However, further detailed investigations are needed to verify whether or not secondary relaxation times can be correlated with the crystallization time scales via Eq. (8).

Table 1. Selected results of the correlation studies based on Eq. (8)

Material	Liquid state (T>Tg)		Glassy state (T<Tg)		Molecular mobility well correlated with crystallization	Ref.
	ξ_X	correlated values	ξ_X	correlated values		
celecoxib	**0.7-0.75**	τ_{cr} with τ_α			α-relax (T>T_g)	65
sildenafil	0.49 0.50	τ_{cr} with τ_α t_0 with τ_α				100
griseofulvin	0.56	τ_{cr} with τ_α	0.19	τ_{cr} with $\tau_{\alpha(\ EAG)}$		67
	0.65	τ_{cr} with τ_α	**0.94** 2.6	$t_{c(0.5\%)}$ with $\tau_{\alpha(EAG)}$ $t_{c(0.5\%)}$ with $\tau_{\beta\text{-}JG}$	α-relax (T<T_g) –	13
nifedipine	0.62 0.82	$t_{c(10\%)}$ with τ_α $t_{c(10\%)}$ with D_{trans}	**0.94** 1.8	$t_{c(10\%)}$ with $\tau_{\alpha(EAG)}$ $t_{c(10\%)}$ with τ_β	α-relax (T<T_g) –	13
nifedipine-(2.5%)PVP	0.67	t_c(10%) with τ_α	**1.2**	$t_{c(10\%)}$ with $\tau_{\alpha(EAG)}$	α-relax (T<T_g)	13
nifedipine-(5%)PVP	0.73	t_c(10%) with τ_α			α-relax (T>T_g)	145
nifedipine-(10%)PVP	0.72	t_c(10%) with τ_α			α-relax (T>T_g)	145
nifedipine-(5%)PVP	0.5	t_0 with τ_α				146
phenobarbital	0.67	t_0 with τ_α				146
phenobarbital-(5%) PVP	0.32	t_0 with τ_α				146
itraconazole	**0.94** 0.68	t_0 with τ_α τ_{cr} with τ_α			α-relax (T>T_g) –	68
trehalose (freeze-dried)	**1.23**	t_0 with τ_α			α-relax (T>T_g)	69
trehalose (spray-dried)	**1.13**	t_0 with τ_α			α-relax (T>T_g)	69
trehalose (dehydrated)	**1.18**	t_0 with τ_α			α-relax (T>T_g)	69
indomethacin	**0.85** 0.29	CGR with τ_α t_0 with τ_α			α-relax (T>T_g) –	63
felodipine	0.43	CGR with τ_α				63

	0.26	t_0 with τ_α				
flopropione	0.20	t_0 with τ_α				63
nifedipine	0.41	CGR with τ_α				63
ketoconazole	0.35	CGR with τ_α				63

$\tau_{\alpha(EAG)}$ – structural relaxation predicted below T_g from extended AG model
τ_{cr} – inverse overall crystallization rate
$t_{c(0.5\%)}$ – characteristic crystallization time obtained for 0.5% degree of crystallization
$t_{c(10\%)}$ – characteristic crystallization time obtained for 10% degree of crystallization
t_0 – crystallization onset time
CGR – crystal growth rate

Besides the correlation studies based on Eq. (8), a straightforward comparison of the time scales of crystallization and relaxation processes is performed to predict the physical stability of amorphous pharmaceutical solids at the storage temperature that is below their glass transition temperatures. For instance (see Fig. 9), it has been found that the time scale of structural relaxation of celecoxib predicted by constructing the master plot (see Section 3.1.2.1) at the room temperature $T_{RT}<T_g$ (τ_α=110h) is in a very good agreement with the storage time at which the maximum rate υ_{max} of the recrystallization of amorphous celecoxib occurs ($t_{c(\upsilon_{max})}=100$h) [11]. Similarly, the time scale of α-relaxation predicted from the master plot construction for ezetimibe, τ_α=22h at $T_{RT}<T_g$, well corresponds to the crystallization onset time for glassy ezetimibe, t_0=14h at T_{RT} [66]. It indicates that the α-relaxation can play an important role in the devitrification of the drugs. Nevertheless, the molecular mobility reflected in secondary relaxations characterized by much faster molecular motions (e.g., for celecoxib, τ_β =0.02s, τ_γ =3μs at T_{RT}) can also affect the recrystallization of the amorphous drugs. If the crystallization time scale of a glassy pharmaceutical were considerably shorter than the time scale of α-relaxation, only secondary relaxations should be considered as factors responsible for the devitrification process.

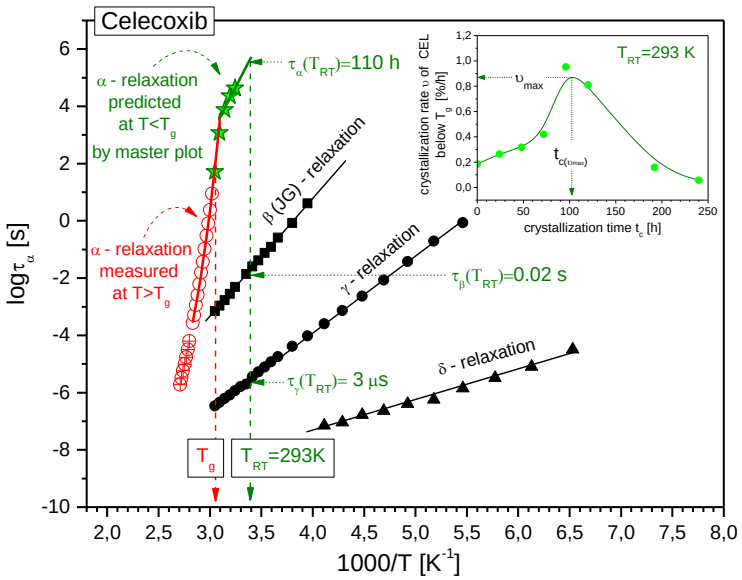

Fig. 9 Plot of temperature dependences of dielectric relaxation times for structural and three secondary relaxation processes of celecoxib. The time scale of the global mobility predicted in the glassy state by constructing the master plot (green stars) is compared with those measured for the various local mobility reflected in secondary relaxations of amorphous celecoxib at the room temperature T_{RT}=293K as well as with the crystallization rate shown in the inset. All data taken from Ref. [11].

3.2 Secondary relaxations

A potential influence of the local mobility reflected in secondary relaxations on the physical instability of amorphous drugs have been suggested for a few reasons [147]. Two of them are especially worth noting: (*i*) the unsatisfactory explanations provided only based on the global mobility for the crystallization kinetics of various pharmaceutical materials both above and below their glass transition temperature and (*ii*) the crystallization phenomena that may occur even at temperatures less than T_g-50K, for which a common belief has been long held that the molecular mobility effect on the physical instability of glasses is negligible (at such low temperatures, the time scale of structural relaxation is extremely long, and then the global mobility seems to be irrelevant to the crystallization process). Nevertheless, it should be noted that the global molecular mobility governs the glass formation and undoubtedly dominates molecular dynamics near the glass transition. Therefore, a lot of attention has been paid to study the intermolecular local mobility reflected in the JG secondary relaxation, which is regarded as a precursor of the structural relaxation and often considered as the most important kind of the local mobility responsible for the recrystallization of glasses. In this context, a proper identification of the JG relaxation among other secondary processes in dielectric spectra is of great importance. Based on the extended coupling model (CM) [132], a useful criterion has been proposed [52] to classify secondary relaxations according to their inter- or intramolecular character, which enables to distinguish between JG and non-JG secondary processes in both dielectric spectra and maps of relaxation times.

In the extended CM model, it is assumed that there is a characteristic microscopic time t_c, independent of thermodynamic conditions, which distinguishes between the dynamic regimes of the non-cooperative and cooperative molecular motions. In the time domain below t_c, molecules relax independently with the characteristic primitive (non-cooperative) relaxation time τ_p, according to the Debye relaxation function: $\phi(t) = \exp\left(-t/\tau_p\right)$. Whereas, at $t>t_c$, the molecules interact in a cooperative manner with the cooperative relaxation time τ_α, according to the KWW function $\phi(t) = \exp\left[-\left(t/\tau_\alpha\right)^{\beta_{KWW}}\right]$ (see Eq. (5)). Then, the primitive relaxation

time τ_p can be derived from the continuity condition at $t=t_c$ as follows $\tau_p = t_c^{1-\beta_{KWW}} \tau_\alpha^{\beta_{KWW}}$, where $t_c \approx 2$ps has been found [148,149,150] for small molecular and polymeric glass formers from quasielastic neutron scattering. Since the JG relaxation is regarded as the precursor of structural relaxation, its relaxation time τ_{JG} should well correspond to the primitive relaxation time τ_p, i.e., $\tau_{JG} \approx \tau_p$. In this way, one may classify a secondary relaxation observed in dielectric spectra as the JG β-process if its relaxation times satisfy the following criterion,

$$\tau_{JG} \approx t_c^{1-\beta_{KWW}} \tau_\alpha^{\beta_{KWW}} . \quad (9)$$

Otherwise, the examined secondary relaxation is a non-JG process (or a pseudo-JG relaxation involving both intra- and intermolecular motions, which has been suggested as an effect of hydrogen bonding [52]). It is worth noting that Eq. (9) can be easily employed in the frequency domain simply considering that $f_{JG} = 1/2\pi\tau_{JG}$ is the frequency at which the JG relaxation loss spectrum reaches its maximal value (see Fig. 10).

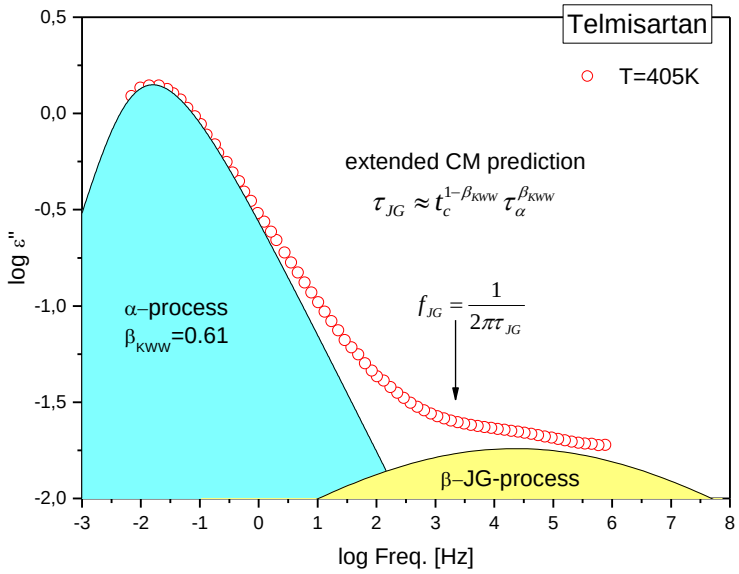

Fig. 10 Illustration of the identification of the JG relaxation in the dielectric loss spectra (data taken from Ref. [93])

The JG relaxation process as a key factor responsible for the recrystallization (both nucleation and crystal growth) deep in the glassy state was proposed by Oguni et al. [151,152,153,154,155,156] based on calorimetry and optical microscopy studies of organic molecular glasses. Striking results reported by the authors [153] were detections of nucleation in 3,3'-dimethoxy-4,4'-bis(2,2-diphenylvinyl) biphenyl about 175K below T_g and even 220K below T_g in another organic glass former (2,2'-dihydroxybenzophenone) [157], where the

latter finding was well accompanied with the dielectric secondary relaxation occurring in the nucleation temperature region.

It should be noted that the actual roles of global and local mobility in inducing the recrystallization of amorphous materials as well as the JG process as a universal feature of all glass formers are still fervently debated. As an argument for no effect of the JG secondary relaxation on the recrystallization process in the glassy state, some examples of materials are given, which recrystallize in the glassy state, although they do not reveal any evidence for the JG process in dielectric spectra (as suggested for 5-methyl-2-[(2-nitrophenyl)amino]-3-thiophenecarbonitrile (ROY) [158]) or exhibit the JG relaxation that disappears in the glassy state too quickly with time to be related to crystal growth (as deduced for ortho-terphenyl (OTP) [159]). Nevertheless, the conclusions rejecting any influence of the JG relaxation on recrystallization in the glassy state seem to be premature due to insufficient experimental evidences taken into account. In this context, a few difficulties in experimental observations of the JG process should be noted. (i) As already mentioned, the amplitude of JG β-relaxation peak is often much smaller in comparison with that of α-relaxation. In these cases, the β-peak can be hidden under the high frequency flank of the structural relaxation peak due to a strong coupling between α- and JG-relaxations, and then an excess wing is observed in dielectric spectra (see Fig. 3). (ii) The JG process is not well detectable by using each experimental technique. For instance, if small dipole moments are assigned to relaxing entities that contribute to the JG relaxation, a weak or no response of the intermolecular local mobility is detected by means of the dielectric spectroscopy. This is the case of OTP, for which a well resolved β-process has been found by using the adiabatic calorimetry [160], while the JG relaxation only can be barely observed by means of the dielectric spectroscopy after rapid quenching and can disappear on annealing [161]. (iii) Thus, the experiment rate may affect the possibility of the JG-process detection. It has been suggested that materials for which no β-relaxation has yet been observed would simply have to be quenched faster in order to give rise to a β-peak [161]. In the light of presented experimental limitations, one cannot exclude the role of the JG relaxation in the recrystallization process especially deep in the glassy state. Therefore, a good practice that has already become a standard research procedure is to always consider the possible influence of the precursor of structural relaxation on the devitrification of amorphous pharmaceutical solids.

An additional rationale for such investigations has been very recently provided by THz spectroscopy studies, which enable to probe fast molecular dynamics of amorphous drugs.

Sibik et al. suggested [162] that the librational-vibrational modes of a series of polyhydric alcohols measured in the THz frequency range are well coupled to the structural and JG secondary dielectric processes observed by standard BDS techniques. Investigating a wide temperature range (well below and above T_g) available by the THz time domain spectroscopy technique, the authors argued that additional thermally dependent contributions to the fast molecular dynamics observed in the temperature range, $0.65T_g<T<T_g$, are related to the JG secondary relaxation, while the dielectric losses at THz frequencies become dominated by the structural relaxation process above T_g. Further, Sibik et al. [163] studied a few pharmaceutical materials at THz frequencies, finding differences in the temperature ranges $T_\beta<T<T_g$ in which the increasing mobility related to the JG relaxation was observed for examined amorphous drugs (i.e., the ratio T_β/T_g varied from 0.55 to 0.76 as well as the different levels of the JG relaxation contribution to the fast molecular dynamics were established for different drugs). Based on these results, a strong correlation between the increase in the fast molecular dynamics and the crystallization onset has been suggested as a promising way to predict the stability of amorphous pharmaceutical solids. It is worth noting that the fast molecular dynamics study probed by the THz spectroscopy has been identified [164] as the caged molecule dynamics, showing up in dielectric spectra as a nearly constant loss (NCL). The regime of caged molecule dynamics is terminated by the onset of the primitive relaxation, which is assumed by the coupling model and can be regarded as a precursor of the JG β-relaxation. Hence, one can establish a connection between the magnitude and the temperature dependence of the NCL and the JG relaxation, which explains a monotonic increase of NCL with temperature and the change to a stronger dependence of dielectric loss observed in the THz spectroscopy in the sub-T_g region, $T_\beta<T<T_g$. Moreover, the temperature T_β has been found as a "second glass transition", because τ_{JG}=100s at T_β, while τ_α=100s at T_g. The consistent description suggested for the molecular mobility investigated in the extremely wide frequency range (from mHz to THz) facilitates a better understanding of the potential relationship of the local molecular mobility and the tendency of amorphous solids to recrystallization.

In recent years, the local motions reflected not only in the intermolecular JG relaxation but also in the secondary relaxations originating from intramolecular motions have been increasingly considered as factors that govern the recrystallization of amorphous pharmaceutical solids. In this context, indomethacin is a model drug that is worthy of discussion. Different kinds of molecular mobility have been thoroughly investigated as

potential factors of the physical instability of the drug that recrystallizes both above and below T_g. Bhugra et al. [63] established that the crystal growth in contrast to the nucleation is quite well coupled with the diffusion process probed by the structural dielectric relaxation in indomethacin above T_g (see Table 1). By comparing the critical size of crystallization nucleus and the dynamic length scale of structural relaxation (see Section 3.1.1), Vyazovkin and Dranca [117] suggested that the crystal nucleation in amorphous indomethacin may occur via the local noncooperative motions of the individual molecules in the temperature region of the secondary β-relaxation. The authors also showed [165] that crystal nuclei began to form in amorphous indomethacin deeply in the glassy state at $T \approx T_g - 56K$ after 147 days of physical aging. Carpentier at al. [166] studied molecular dynamics of indomethacin using dielectric and NMR spectroscopies, reporting a presence of two secondary relaxations in the glassy state. The slower β-relaxation was classified as the JG process in terms of Eq. (8) based on the extended CM, and the faster γ-relaxation was attributed to intramolecular motions (the chlorobenzyl group rotations detected in NMR measurements). Both the interpretations have been later confirmed by finding better resolved JG β-relaxation peaks in dielectric spectra of amorphous indomethacin measured at elevated pressure (P=400MPa) and giving evidence that the non-JG γ-relaxation is insensitive to pressure [167]. Based on the NMR measurements carried out for metastable and stable crystalline phases of indomethacin, a possible scenario has been suggested that the mobility inducing the crystal nucleation far below T_g comes from the combined effects of the JG secondary relaxation and the chlorobenzyl group rotations [166].

The case of indomethacin shows that thorough investigations of all secondary processes observed in the glassy state of pharmaceuticals are important to exhaustively determine molecular mechanisms that govern the complex recrystallization phenomenon. The role of intramolecular relaxations in predicting the physical stability of glasses can be especially exposed if specific interactions (e.g. hydrogen bonds) exert an essential effect on the tendency of amorphous drugs to recrystallization. Considering another important issue, which is the influence of water on the susceptibility of amorphous drugs to recrystallization, we need to remember that water contained in a material not only results in its plasticization (i.e., an increase in the global mobility associated with a decrease in T_g of the hydrated material), but also affects the local mobility of the material. After adding water to a material, a new relaxation process originating from local motions of water molecules begins to emerge in the frequency range typical for secondary processes [85,168], which makes the local molecular dynamics of hydrated drugs more complex than their anhydrous counterparts. The enhanced

global and local mobility of hydrated materials are usually correlated with their higher tendency to crystallization. However, it was also reported that water can act as an antiplasticizer for local motions [147]. For instance, an increase in the water content caused an increase in the activation energy of β-relaxation in poly(vinylpyrrolidone) [169]. Thus, both single pharmaceuticals and pharmaceutical mixtures require individual investigations to properly assess the influence of their molecular mobility on their physical stability.

4. Enhancement of the physical stability of amorphous drugs

A growing interest in advantages of amorphous drugs (i.e., their better solubility and consequently bioavailability) over their crystalline counterparts has resulted in many attempts to find effective and efficient methods for preparing amorphous pharmaceutical solids, which will be physically stable upon their storage (at least during their shelf life) and after administration. A very promising way to achieve this goal is to prepare amorphous compositions of APIs with certain excipients (including both polymers and small molecule compounds, which are crystallization inhibitors) as well as amorphous binary mixtures of two different APIs. In search of ideal excipients that are not APIs to such applications, the additives are preferred, which are sufficiently effective at the lowest possible concentration to physically stabilize amorphous drugs.[145]

The enhancement of the physical stability of amorphous APIs by mixing them with excipients has been originally based on the antiplasticization effect of the added material on API, i.e., a decrease in the global mobility associated with an increase in T_g of the binary system compared with that of the pure API. This strategy consists in the preparation of mixtures of a drug with an excipient having a higher T_g than that of the drug. In a typical case, the mixing of two materials results in the glass transition temperature of their binary mixture, which can be described by the Gordon-Taylor (GT) equation [170]:

$$T_g(x) = \frac{xT_{g1} + K(1-x)T_{g2}}{x + K(1-x)}, \qquad (10)$$

where x is the mass fraction of the component 1, T_{g1} and T_{g2} are respectively glass transition temperatures of the components 1 and 2, whereas *K* is a fitting parameter, which can be interpreted as a measure of interactions between components and described for instance by the ratio of changes in the heat capacities of the components at their glass transition temperatures, $\Delta C_{p2}/\Delta C_{p1}$.[171] If a drug characterized by its glass transition temperature T_{g1} is mixed with another component having its glass transition temperature $T_{g2} > T_{g1}$, then Eq. (10) predicts

that the glass transition temperature of the mixture will be higher than the glass transition temperature of the pure drug ($T_g(x) > T_{g1}$). As a result, the molecular mobility of the prepared mixture is reduced in comparison with the pure drug, thereby one can expect a lower tendency of this amorphous binary system to devitrification. Therefore, the commonly used excipients in mixtures with drugs are polymers often characterized by high values of T_g.

However, the strategy of the physical stability improvement based on Eq. (10) is not universal, because the glass transition temperature is not always a proper predictor of the tendency to recrystallization. Similarly to single component pharmaceutical systems, there are known amorphous binary systems characterized by nearly the same values of T_g and different tendencies to recrystallization. For example, amorphous nifedipine crystallizes more readily than amorphous felodipine, although their values of T_g are very close, i.e., (45.5±0.3)°C for nifedipine and (46.4±0.3)°C for felodipine. The crystallization tendency compared between these drugs do not change in the presence of 3 wt% polyvinylpyrrolidone (PVP) [21]. If different polymers characterized by nearly the same value of T_g are added to the same API, they can also exert different effects on the physical stability of the amorphous pharmaceutical systems. For example, poly(acrylic acid) (PAA) better prevents the recrystallization of acetaminophen than PVP, although the values of T_g for PAA and PVT are almost identical, resulting in very close values of T_g for amorphous solid dispersions ((30.3±0.3)°C for acetaminophen with PVP and (31.3±0.5)°C for acetaminophen with PAA) [172]. Moreover, predictions given by Eq. (10) can be considerably different from experimental values of T_g obtained for amorphous binary systems. The breakdown of the GT equation is usually argued by specific intra- and intermolecular interactions (e.g. hydrogen bonds and ionic interactions), which can be essential to facilitate or hinder the formation of crystal nuclei and/or the crystal growth [173,174]. Thus, an alternative strategy for the selection of excipients to amorphous solid dispersions containing drugs relies on finding such additives, the molecules of which are able specifically interact with API molecules to prevent the recrystallization process [175,176,177,178,179, 180,181].

In current pharmaceutical investigations, a combined influence of antiplasticization (generally understood as a decrease in the global or/and local molecular mobility [147]) as well as specific interactions on the physical stability of amorphous solid dispersions is most often considered to effectively suppress their recrystallization. For instance, Kothari et al. [182] investigated a possible role of drug-polymer H-bonding interactions and molecular mobility on the physical stability of nifedipine dispersions with polymers such as PVP, PAA,

and hydroxypropylmethyl cellulose acetate succinate (HPMCAS). As a result, the authors have found that the strength of drug-polymer hydrogen bonding, the increase in structural dielectric relaxation times of the dispersions, and the resistance to crystallization can be ranked depending on polymer additives as follows PVP > HPMCAS > PAA (compared at two polymer concentrations of 10 and 20 wt% in the drug dispersions). The best effectiveness of PVP in stabilizing nifedipine in the amorphous binary compositions has been attributed to the decrease in molecular mobility caused by the strong hydrogen bonding between molecules of PVP and nifedipine. An interesting comparison of the roles of antiplasticization and hydrogen bonding in the physical stabilization can be drawn for amorphous mixtures of celecoxib with the polymer PVP[183,184] and a small molecule compound octaacetylmaltose (acMAL) [8]. For the amorphous binary mixture of celecoxib with PVP, a strong antiplasticization effect has been observed, however, the increase in T_g of the amorphous mixture with increasing content of PVP has not complied with the predictions based on the GT equation. This deviation from the dependence $T_g(x)$ estimated by Eq. (10) has been explained by hydrogen bonding between the $–NH_2$ group of celecoxib and the –C=O group of PVP. In the physical stabilization of amorphous celecoxib by mixing with acMAL, the antiplasticization effect does not play any role if it is considered in the conventional sense, because the glass transition temperatures of celecoxib and acMAL have the same value (T_g=331K). Indeed, there is no increase in T_g of the amorphous binary systems compared with its drug component, and even the values of T_g of celecoxib-acMAL mixtures are slightly lower than that for pure celecoxib. Nevertheless, after adding cMAL to celecoxib, some changes occur in the global mobility compared with that of pure celecoxib, which are reflected in a decrease in the isobaric fragility *m* determined from Eq. (4) using dielectric data (see Fig.11). The drop in the isobaric fragility well corresponds to the enhanced physical stability of the co-amorphous binary system in the liquid state, which is in accord with the general expectations that stronger materials should be more stable as well as with the predictions of the TOP model formulated by Tanaka (see Section 3.1.1). However, no crystallization tendency of the co-amorphous solid dispersion of celecoxib with acMAL has been mainly attributed to a significant suppression of both the intermolecular and intramolecular local mobility of pure glassy celecoxib after mixing with acMAL. Based on the broadband dielectric spectroscopy studies and the density functional theory calculations, it has been established that even a small content of acMAL (10wt%) in the glassy binary mixture with celecoxib causes a slowdown in the JG β-relaxation as well as a rapid decrease in the dielectric strength of a non-JG γ-relaxation due to arresting rotations of the –phenyl-$SONH_2$ group of celecoxib (which are responsible for the γ-process) by strong

hydrogen bonds formed between the –phenyl-$SONH_2$ group of celecoxib and the –C=O group of acMAL. The pioneering application of acMAL to effectively stabilize amorphous celecoxib [8] has inspired further successful attempts [185, 186] at exploiting acetylated saccharides as crystallization inhibitors of other amorphous pharmaceuticals.

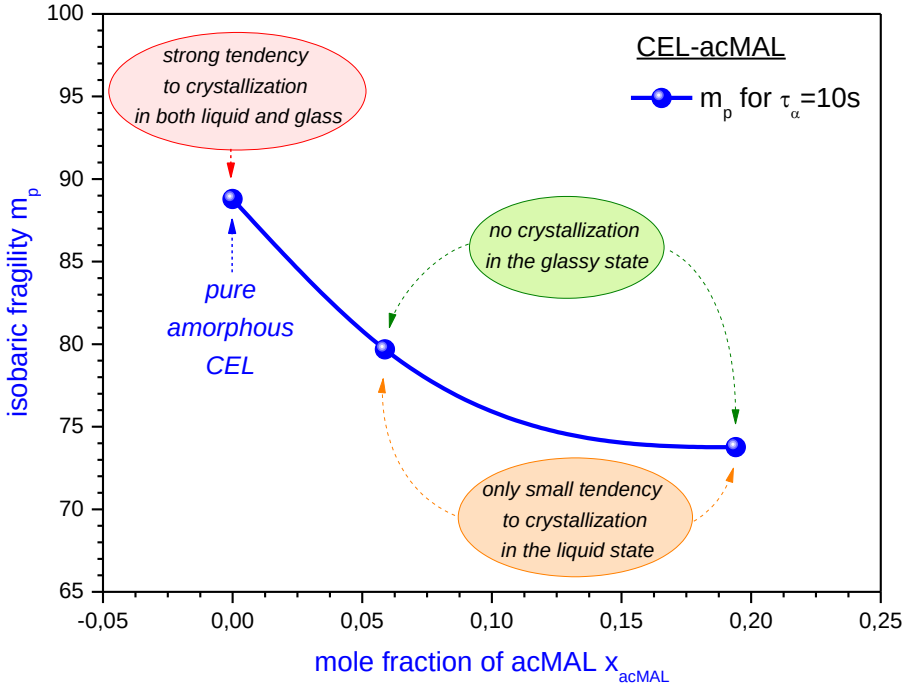

Fig. 11 Example of a correlation between the significant enhancement in the physical stability and the decrease in the isobaric fragility after adding a small amount of octaacetylmaltose (10% and 30% wt of acMAL) to celecoxib (CEL). Data are taken from Ref. [8].

In search of excipients effectively preventing the recrystallization of amorphous pharmaceutical solids, an active interest has been taken in studying additives that can stabilize amorphous APIs via ionic interactions. Mistry et al. [175] have suggested that a further enhancement in the physical stability may be achieved in case of ionic interactions between molecules of drug and excipient, because such interactions are stronger than hydrogen bonding. The authors investigated ketoconazole solid dispersions with three polymers such as PVP, PAA, and poly(2-hydroxyethyl methacrylate) (PHEMA), finding that the strength of drug - polymer interaction, the increase in dielectric α -relaxation times, and the enhancement in physical stability (crystallization inhibition) can be ranked depending on polymeric excipients in the following order: PAA > PHEMA > PVP. These results have been elucidated by ionic interactions and hydrogen bonding between ketoconazole and PAA as well as hydrogen bonding and weaker dipole-dipole interactions of ketoconazole with PHEMA and

PVP. The strong ionic interactions have been attributed to a huge decrease in the global mobility of ketoconazole-PAA binary systems with increasing polymer concentration as well as to a delay in the crystallization onset temperature and the crystallization process. Using dimethylaminoethyl methacrylate copolymer, Liu et al. [187] successfully stabilized indomethacin due to suppression of the indomethacin dimer formation via ionic interactions between the drug and the copolymer. There are also known applications of inorganic silicates to enhance the physical stability of amorphous drugs, in which the important role of ionic interactions is also suggested.[188,189,190, 191, 192, 193, 194,195]

A tempting idea to enhance the physical stability of amorphous drugs is to prepare amorphous mixtures of two different APIs. The first attempts to combine two amorphous drugs with one another were made by Yamamura *et al*. [196]. In 1996, the researchers first formed an amorphous binary composition of the nonsteroidal anti-inflammatory drug (NSAID) naproxen with cimetidine used in the treatment of heartburn and peptic ulcers. A few years later, the same group prepared the drug mixtures containing cimetidine and indomethacin (NSAID) both in their disordered state [197]. Spectroscopic studies show that the formation of amorphous cimetidine/naproxen and cimetidine/indomethacin compositions was possible due to non-bonding intermolecular interactions between the imidazole ring of cimetidine and the carbonyl group of the naproxen or indomethacin.

In 2009, Alleso et al. discovered that an amorphous mixture of two drugs cimetidine and naproxen indeed enhanced the dissolution rate of both substances compared to their crystalline counterparts.[198] In the same year, Chieng et al. [199] showed that the amorphous composition of indomethacin with ranitidine is characterized by a much better physical stability than those of the pure amorphous drugs. In 2011, Löbmann et al. prepared and investigated the amorphous mixture containing two NSAIDs: naproxen and indomethacin at different molar ratios (2:1, 1:1 and 1:2) [200]. Both the x-ray powder diffraction (XRPD) and the differential scanning calorimetry (DSC) studies proved that naproxen in binary amorphous drug-drug mixture with indomethacin could be made amorphous, whereas pure naproxen could not be amorphisized due to its very high tendency to crystallization. Additionally, the authors observed a substantial increase in the intrinsic dissolution rate of indomethacin in the mixture compared to the crystalline form of pure indomethacin. The authors also achieved an improvement of dissolution rate of glipizide upon formation of co-amorphous simvastatin/glipizide mixtures [201], where glipizide acts as an anti-plasticizer and raises the glass transition temperature of the simvastatine and stabilizes the amorphous mixture.

Indomethacin was also studied in composition with ranitidine hydrochloride and ritonavir in the same drug – drug ratio. The stability of amorphous forms in both formulations were identified during the storage periods of 30 and 90 days respectively [199,201]. Martinez L. *et al* [202] obtained very stable binary system paracetamol-antypiryne in a very wide range of temperatures (-50º to 160ºC) and without any sign of crystallization even after storage longer than one year at room temperature. The latest investigations show that even a small amount of indapamid (8.8wt%) that reveals a low tendency to crystallization alone is able to suppress the recrystallization of amorphous ezetimibe [203]. The co-amorphous mixture of ezetimibe and indapamid has remained physically stable even after 72 days of storage at room temperature. This resistance against recrystallization significantly enhanced by mixing ezetimibe with indapamid has been suggested to result from the anitiplasticization effect exerted by indapamid. The slowdown in the molecular mobility of co-amorphous binary mixture with increasing indapamid content has been well described by the GT equation (Eq. (10)) and well correlated with a decrease in the isobaric fragility determined from Eq. (4) by using dielectric experimental data.

Co-amorphous compositions of two drugs are extremely interesting also because of their medical advantages. Namely, it has been many times reported that the combination therapy of two drugs gives better results than monotherapy [204,205,206]. Since the vast majority of medical papers consider compositions of two crystalline drugs, there is a clear need for improving the solubility and bioavailability of these mixtures by converting the crystalline binary compositions into their amorphous forms.

5. Crystallization of amorphous drugs at elevated pressure

As already mentioned in previous sections, the interest in studying the crystallization of supercooled and glassy pharmaceutical systems at high pressure is driven by compression paths used to prepare tablets of API and formulations, showing often a very complex inhomogeneous scenario [38]. On the other hand, the possibility to change simultaneously and independently molecular thermal energy and density offers an additional tool to investigate the role of dynamics and thermodynamics in determining the tendency to recrystallization and explore its behavior through the T-P diagram. For instance, a possible line of future investigations, which has been recently started [207,208], is the study of the possible role of polymorphs and their influence on the stability of amorphous state over the T-P plane. In recent years, there is a growing interest in studies combining pressure and temperature

variations since they allow to affect thermodynamic and dynamic properties for a given system in quite different ways. With this respect, the broadband dielectric spectroscopy is a unique technique to monitor both dynamics and real-time crystallization kinetics at high pressure. In fact, classical techniques to monitor crystallization, such as X-ray diffraction, differential scanning calorimetry and infrared absorption (FTIR) are usually employed to study the amount of crystallized phase (and so the stability) of amorphous systems created off-line at high pressure [38, 209], but very few studies have been performed directly on-line at very high pressure, mainly exploiting calorimetric, volumetric and FTIR techniques [208, 210, 211]. The broadband dielectric spectroscopy can be easily performed at high pressure, giving access to both dynamics and crystallization kinetics. In fact, in most of the cases, when supercooled molecular systems start to crystallize, only the amorphous phase contributes to the dielectric response, being the dielectric strength $\Delta\varepsilon$ proportional to the number of active dipoles per volume unit. In absence of additional mesophases or confined amorphous phases that could bear additional effects and prevent a simple analysis [212], the amount of crystallization fraction can be estimated directly from dielectric spectra using the following relations exploiting a normalized change in the dielectric dispersion $\varepsilon'_N(t)$,

$$\alpha(t)=\varepsilon'_N(t)=1-\frac{\Delta\varepsilon(t)}{\Delta\varepsilon(0)}=1-\frac{\varepsilon'(t)-\varepsilon'(\infty)}{\varepsilon'(0)-\varepsilon'(\infty)}=1-\exp\left[-(kt)^n\right] \qquad (11)$$

where the conversion degree α is a measure of how rapidly active dipoles decrease during the crystallization process. The last term is the Avrami function [213, 214], where *k* that is the overall crystallization rate constant (related to both nucleation and growth and corresponding to the characteristic overall crystallization time $\tau_{cryst}=k^{-1}$) and *n* is the Avrami exponent often correlated with the nature of crystal growth. The Avrami function may bear also an offset time term t_0, related to the onset of crystallization if *t* is replaced with t-t_0. Samples can be melted at high pressure, then cooled to the target temperature to be monitored isothermally. In Fig.12 and 13 there are some examples of monitoring the crystallization kinetics for amorphous drug probucol [215] and indomethacin [39].

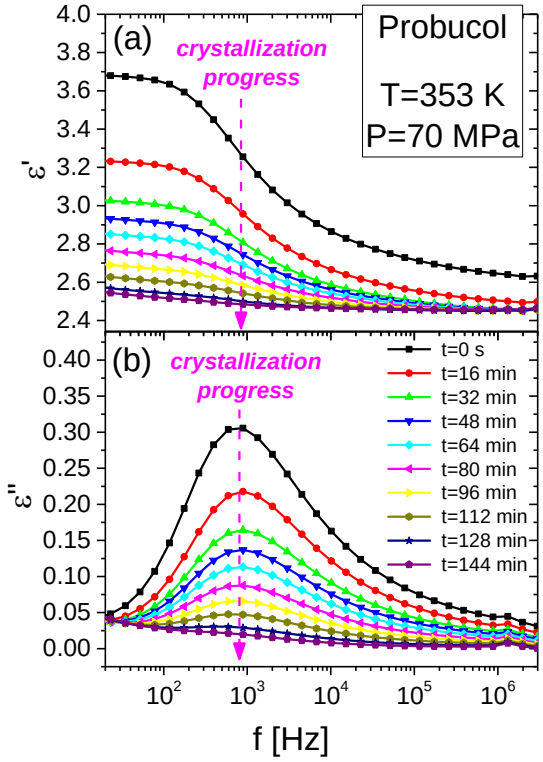

Fig. 12 Real (a) and imaginary (b) part of permittivity of probucol at 353 K and 70 MPa. Isothermal spectra acquired at different times are shown.

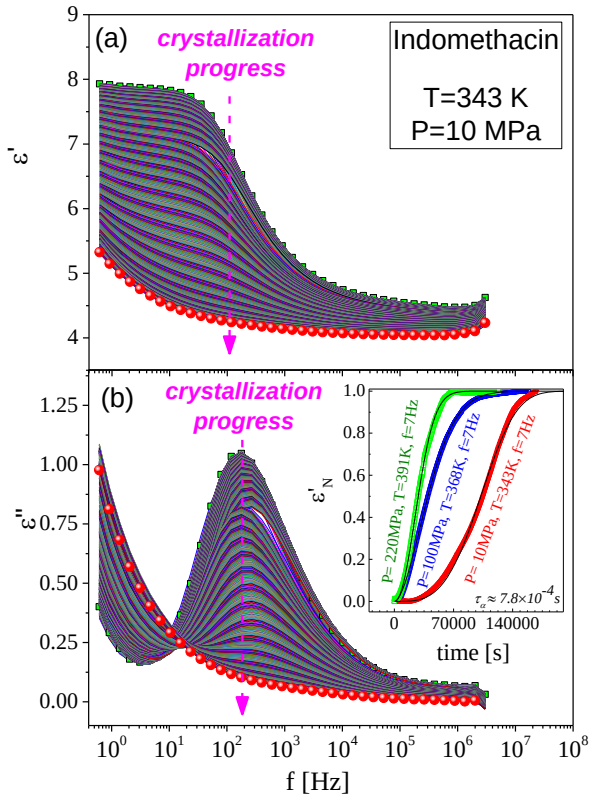

Fig. 13 Real (a) and imaginary (b) part of permittivity of indomethacin at 329 K and 1057 MPa [39]. Inset shows the crystallinity fraction as obtained from eq.11 at different T and P conditions.

The possibility to access simultaneously to dynamics (from the relaxation times obtained from the frequencies of the dielectric loss peak maxima) and to crystallization kinetics allow to test also the previously mentioned Eq. (8) also at high pressure. An examples can be found in Figure 14 for probucol at 353 K and different pressures where the crystallization rate and the reciprocal α-relaxation times are compared [215].

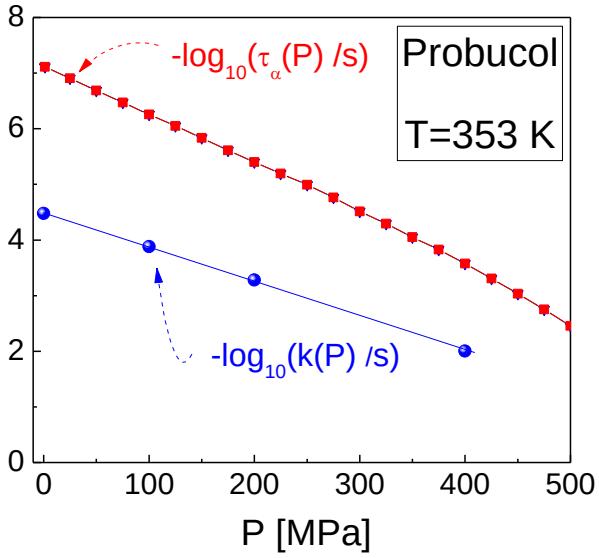

Fig. 14 Logarithm of inverse crystallization rate ($k^{-1} = \tau_{cryst}$) and inverse relaxation time for probucol at 353 K plotted versus pressure.

The crystallization times as well as the relaxation ones increases on increasing density and keeping temperature constant. That is expected, since the molecular mobility is quite reduced on increasing density, but actually the relaxation times seem to be more affected than the crystallization rate. The possibility that this result could be related to a different dynamic variable to which the crystallization growth or nucleation is coupled has already been mentioned in this paper. On the other hand, we have to consider here that, on changing density, all the excess thermodynamic quantities, including entropy and free energy are reduced on increasing density. The tempting idea could be that, on changing pressure at suitable temperature, less or more stable amorphous state could be obtained.

The recent years have seen a flourished series of papers studying the crystallization kinetics at different pressures by dielectric spectroscopy [12,39,40,41,216,217]. If a rationale can be found about the stability against recrystallization (or the instability) at high pressure, the suitable T-P conditions should be chosen to effectively perform such stability investigations. It has been shown [19,102] that in most glass-forming systems, despite the

pressure or temperature conditions, once a fixed structural relaxation time τ_α(T,P) is chosen, all the dynamic results are very similar. In other terms, in isochronal conditions (i.e., at τ_α(T,P)=const) the shape of α-relaxation peak (hence the distribution of structural relaxation times), the coupling between the structural relaxation times τ_α and the JG-relaxation times τ_β [218,219], and the decoupling exponent between translational and rotational diffusion coefficient remain unchanged [19]. These findings have been rationalized by a couple of models. For instance, we have already introduced the Coupling Model by Kia Ngai [20], according to which all dynamic quantities are invariant at selected T and P at which the primitive relaxation time τ_p is kept constant. Thus, one can suggest that a good choice is to perform the kinetics studies in the same isochronal conditions defined at the same τ_α(T,P) or the same τ_p(T,P). Another support can come from the theory of isomorphs [220], which predicts the possibility to find such state points that can be isomorphically transformed one into the others, providing curves in the T-P diagram called isomorphs along which various dynamic observables are expected to be invariant despite varying density ρ and temperature T, if it is possible to describe the thermodynamic evolution of a given dynamic observable by a function of the single scaling variable defined originally by the ratio h(ρ)/T, which takes into account the increase in the intermolecular barrier due to the increase in density. Having both the experimental and theoretical supports, the choice of studying the crystallization kinetics in isochronal conditions appears as the best way to investigate the stability of amorphous drugs against recrystallization within the well-defined molecular mobility.

The fundamental advantage of the isochronal method for exploring the crystallization kinetics has been recently elucidated in terms of the classical theory for the crystallization under high pressure and demonstrated using a model drug indomethacin as an example [39]. According to the crystallization theory [17,221,222], the quantities typically used to characterize the crystallization process such as the nucleation rate *I*, the crystal growth rate *g*, and the non-steady-state time lag $\tau_\#$ depend on thermodynamic and kinetic factors and can be expressed by some functions of temperature and pressure in the following way,

$$I(T,P) = C_1 \exp[-\Delta W(T,P)/k_B T]\exp[-U(T,P_0) f_4(P)] \quad (12a)$$

$$g(T,P) = C_2 \Omega[-\Delta\mu\, f_3(P)]\exp[-U(T,P_0) f_4(P)] \quad (12b)$$

$$\tau_\#(T,P) = C_3 \left\{\sigma_0 f_3(P)/[\Delta\mu_o f_2(P)]^2\right\}\exp[U(T,P_0) f_4(P)] \quad (12c)$$

where the parameters C_i are constant, the functions f_i are only pressure dependent, and the thermodynamically governed terms involve the thermodynamic barrier to nucleation, $\Delta W(T,P)$, the specific surface energy of the melt/crystal interface, $\sigma(T,P)$, and the thermodynamic driving force of crystallization, $\Delta\mu(T,P)$, which is the difference in the chemical potentials of the ambient and the newly formed phase. The symbols σ_0 and $\Delta\mu_0$ refer to the normal pressure case and the function $\Omega[-\Delta\mu\, f_3(P)]$ denotes a general expression that can take different forms depending on particular mechanisms of the crystal growth. However, the kinetic contribution to Eqs. (12a)-(12c), which reflects the molecular mobility, is represented by the exponential factor $\exp[-U(T,P_0)\, f_4(p)]$ or its inverse, where $U(T,P_0)$ is the overall activation energy at the normal pressure p_0=0.1MPa. As already mentioned in Section 3.1.2.2, the kinetic factor of the crystallization process is considered to be dependent on the molecular diffusion, and consequently to be related to the inverse viscosity η^{-1} or the inverse structural relaxation time τ_α^{-1} for $I(T,P)$ and $g(T,P)$, while $\tau_\#(T,P)$ is non-inversly dependent on η or τ_α. Therefore, even if the decoupling phenomena discussed in Section 3.1.2.2 may occur, one can assume that the kinetic contribution to the characteristic crystallization quantities $I(T,P)$, $g(T,P)$, and $\tau_\#(T,P)$ is invariant to a good approximation in isochronal conditions, e.g., at $\tau_\alpha(T,P) = const$. Then, the thermodynamic contributions to these quantities can be conveniently extracted by changing pressure along such a defined isochronal curve in the T-P diagram. Among other things, in most examined systems, such studies revealed that the pressure derivative of the crystallization temperature dT_{cr}/dP calculated along an isochrone changes differently (usually less strongly at high P) than the pressure derivative of the melting temperature dT_m/dP along the melting line in the T-P diagram. Thus, the supercooling range $T_m(P)$-$T_{cr}(P)$ increases with increasing pressure. It means that one can presume that keeping the same kinetic barrier upon crystallization process does not guarantee that we are still in the same relative position with respect to the melting point.

The progress made in the crystallization studies by exploiting the isochronal paths has also revealed some limitations in the previous methods for determining the thermodynamic parameters of the crystallization process such as $\Delta\mu(T,P)$ and $\sigma(T,P)$. In the classical approach suggested by Gutzow et al. [17, 221,222] to study the crystallization process at some temperature and pressure (T_{cr},P_{cr}), the integration pathway has been employed (see Fig. 15), which starts from the melting temperature at the normal pressure, $T_m(P_0)$, achieves the

crystallization temperature $T_{cr}(P_0)$ along the isobar P_0, and then isothermally reaches the crystallization state (T_{cr},P_{cr}). Along the pathway, for instance, the difference in the chemical potentials $\Delta\mu(T,P)$ can be determined by the following equation

$$\Delta\mu(T,P) = -\int_{T_m(P_0)}^{T} \Delta S(T,P_0)dT + \int_{P_0}^{P} \Delta V(T_m(P_0),P)dP \qquad (13)$$

where $\Delta S = S_{liq} - S_{cr}$ and $\Delta V = V_{liq} - V_{cr}$ denote the differences in the entropies and volumes of the liquid and crystalline states, respectively. Very recently, it has been shown [40] that the integration pathway employed in Eq. (13) is proper in the cases in which $T_{cr} < T_m(P_0)$ (as presented in Fig. 15(a)), but it becomes inadequate if $T_{cr} > T_m(P_0)$ (as depicted in Fig. 15(b)), because then it requires extrapolating the entropy of crystal to the liquid state, which leads to physically unjustified results as above the melting point the crystalline state does not exist. The newly suggested integration pathway [40] overcomes the essential limitation, because (see Fig. 15(b)) it starts from the same initial point ($T_m(P_0)$,P_0), but first achieves the crystallization pressure P_{cr} along the isotherm $T_m(P_0)$, and then isobarically reaches the crystallization state (T_{cr},P_{cr}). Then, the difference in the chemical potentials can be rewritten as follows

$$\Delta\mu(T,P) = -\int_{T_m(P_0)}^{T} \Delta S(T,P)dT + \int_{P_0}^{P} \Delta V(T_m(P_0),P)dP \qquad (14)$$

It is worth noting that the integration pathway employed in Eq. (14) can be also applied to the cases at which the crystallization temperatures $T_{cr} < T_m(P_0)$. Thus, the thermodynamic driving force toward crystallization typically expressed by the difference between chemical potentials of liquid and crystalline phases, $\Delta\mu$, the liquid/crystal interfacial free energy, σ, also based on the integrals exploited in Eqs. (13) and (14) as well as the critical size of crystallization nucleus r^*, which depends on σ, can be properly evaluated along the new integration pathway as it has been done in [40] successfully exploiting both the commonly used Tait equation of state [223] and the recently derived equation of state [224,225,226] to parametrize the temperature-pressure dependence of volume in order to thoroughly verify the new integration pathway.

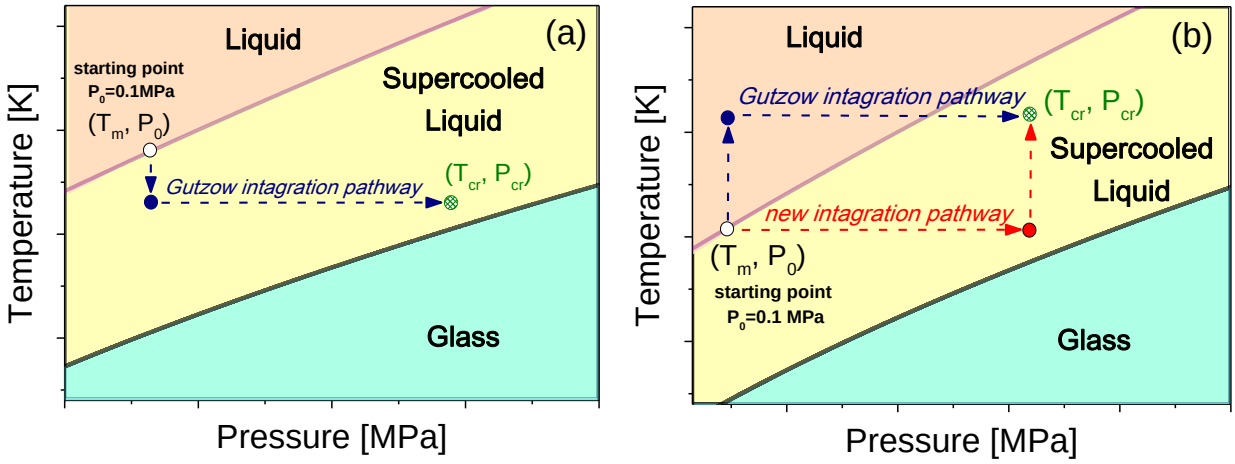

Fig. 15 Illustration of the integration pathways originally suggested by Gutzow et al. [17,221,222] and newly proposed in Ref. 40 to calculate the thermodynamic driving force toward crystallization in two cases (a) $T_{cr} < T_m(P_0)$, and (b) $T_{cr} > T_m(P_0)$. The new integration pathway is not shown in panel (a), although it is also valid at $T_{cr} < T_m(P_0)$.

The extensive studies performed in the last few years show a quite complex scenario. As mentioned previously in this paper, high pressure paths might yield amorphous materials with a higher stability, due to a less excess of free energy, a reduced fragility, a less decoupling, and a larger activation energy for local processes. The effect of density over the thermal fluctuations in favoring fast growth of crystals close to the glass transition temperature, where the sample is viscous and the molecular motions are quite hindered, has been also theorized [227]. Isochronal experiments similarly gave opposite results, with the crystallization rate both strongly reduced (for ibuprofen [12,41]) or enhanced (for ROY) [216] with increasing pressure. In a very recent paper, the crystallization kinetics for racemic and single enantiomers of a pharmaceutical system have been reported to have opposite trends with pressure, i.e., the overall crystallization rate of the single component system increases with compression, while it decreases in case of the racemic mixture [217]. Being the crystallization scenarios very rich, it is important to have a reliable method at our disposal to represent and predict the evolution of the crystallization behavior with pressure and to relate it to dynamics and thermodynamics. It should be noted that there is a competition between these two factors affecting the crystallization kinetics under pressure in a different manner: the mobility term is reduced by density, differently from the other one that can have a complex behavior. Depending on their combination theoretically described by Eqs. (12a)-(12c), the recrystallization of a liquid under compression may be faster or slower. The crystallization

kinetics studied in isochronal conditions and the choice of the proper thermodynamic pathways to analyze the thermodynamic parameters relevant to the recrystallization process enable to reliably assess the variation in the thermodynamic and kinetic contributions to the recrystallization phenomenon.

Conclusions

The recent progress made in studying the physical stability of amorphous APIs undoubtedly shows that the molecular mobility is a key factor that governs the recrystallization process of pharmaceuticals from the glassy state, although it is still difficult to determine which kinds of molecular mobility are responsible for the undesirable devitrification of amorphous drugs in any case. Thus, in the further research perspectives on this field, such investigations should be certainly involved, which are aimed at gaining a better insight into correlations between properties of the different kinds of molecular mobility and the crystallization process. The powerful experimental method for conducting such studies is the broadband dielectric spectroscopy, which enables to examine both molecular dynamics and crystallization kinetics in the wide temperature-pressure range, covering an extremely broad frequency band that enables to reveal the characteristic time scales of different dielectric relaxation processes and crystallization kinetics. Nevertheless, the complex nature of amorphous pharmaceutical solids may most likely require exploring some combinations of both dynamic and thermodynamic various factors to completely understand molecular mechanisms of the devitrification process, and consequently allow us to predict and control the physical stability of amorphous APIs. For this purpose, novel research procedures are expected to be very useful, which are able to reliably distinguish between thermodynamic and kinetic contributions to the examined physicochemical phenomena. In this context, the study of the pressure effect on the molecular mobility and the crystallization kinetics should shed a new light on both application and cognitive aspects of the physical stability of amorphous pharmaceutical solids.

Acknowledgements

M.P. and K.G. are grateful for the financial support received within the Project No. 2015/16/W/NZ7/00404 (SYMFONIA 3) from the National Science Centre, Poland.

References

[1] H.D. Williams, N.L. Trevaskis, S.A. Charman, R.M. Shanker, W.N. Charman, C.W. Pouton, C.J. Porter, Strategies to address low drug solubility in discovery and development. Pharmacol. Rev. 65 (2013) 315-499.

[2] L. Di, P.V. Fish, T. Mano, Bridging solubility between drug discovery and development. Drug Discov Today, 17 (2012) 486-495

[3] D.Q. Craig, P.G. Royall, V.L. Kett, M.L. Hopton, The relevance of the amorphous state to pharmaceutical dosage forms: glassy drugs and freeze dried systems Int. J. Pharm. 179 (1999) 179–207

[4] B.S. Murdande, M.J. Pikal, R.M. Shanker, R.H. Bogner, Solubility Advantage of Amorphous Pharmaceuticals: I. A Thermodynamic Analysis Pharm Res. 27 (2010) 2704-14

[5] B.S. Murdande, M.J. Pikal, R.M. Shanker, R.H. Bogner, Solubility Advantage of Amorphous Pharmaceuticals, Part 3: Is Maximum Solubility Advantage Experimentally Attainable and Sustainable?, J. Pham.Sci. 100 (2011) 4349-4356

[6] K. Adrjanowicz, K. Kaminski, M. Paluch, P. Wlodarczyk, K. Grzybowska, Z. Wojnarowska, L. Hawelek, W. Sawicki, P. Lepek, R. Lunio, Dielectric relaxation studies and dissolution behavior of amorphous verapamil hydrochloride, J. Pharm. Sci. 99 (2010) 828-839.

[7] B.C. Hancock, M. Parks, What is the True Solubility Advantage data for the melting point, heat of fusion, and heat capacity of for Amorphous Pharmaceuticals? Pharm. Res. 17 (2000) 397-404

[8] K. Grzybowska, M. Paluch, P. Wlodarczyk, A. Grzybowski, K. Kaminski, L. Hawelek, D. Zakowiecki, A. Kasprzycka, I. Jankowska-Sumara, Enhancement of amorphous celecoxib stability by mixing it with octaacetylmaltose: the molecular dynamics study. Mol. Pharm. 9 (2012) 894-904

[9] K. Adrjanowicz, K. Grzybowska, K. Kaminski, L. Hawelek, M. Paluch, D. Zakowiecki, Comprehensive studies on physical and chemical stability in liquid and glassy states of telmisartan (TEL): solubility advantages given by cryomilled and quenched material. Philosophical Magazine, 91 (2011) 1926 – 1948.

[10] K. Kaminski, K. Adrjanowicz, Z. Wojnarowska, K. Grzybowska, L. Hawelek, M. Paluch, D. Zakowiecki, J. Mazgalski, Molecular dynamics of the cryomilled base and hydrochloride ziprasidones by means of dielectric spectroscopy. J. Pharm Sci. 100 (2011), 2642–2657

[11] K. Grzybowska, M. Paluch, A. Grzybowski, Z. Wojnarowska, L. Hawelek, K. Kołodziejczyk, K.L. Ngai, Molecular Dynamics and Physical Stability of Amorphous Anti-Inflammatory Drug: Celecoxib, J. Phys. Chem. B, 114 (2010) 12792–12801

[12] K. Adrjanowicz, K. Kaminski, Z. Wojnarowska, M. Dulski, L. Hawelek, S. Pawlus, M. Paluch, W. Sawicki, Dielectric relaxation and crystallization kinetics of ibuprofen at ambient and elevated pressure; J. Phys. Chem. B. 114 (2010) 6579-93.

[13] K. Kothari, V. Ragoonanan, R. Suryanarayanan, Influence of Molecular Mobility on the Physical Stability of Amorphous Pharmaceuticals in the Supercooled and Glassy States, Mol. Pharmaceutics, 11 (2014) 3048−3055

[14] P. Karmwar, K. Graeser, K.C. Gordon, C.J. Strachan, T. Rades, Investigation of properties and recrystallisation behaviour of amorphous indomethacin samples prepared by different methods, Int. J. Pharm. 417 (2011) 94–100

[15] S. Capaccioli, M. Paluch, D. Prevosto, Li-Min Wang, K. L. Ngai, Many-Body Nature of Relaxation Processes in Glass-Forming Systems, J. Phys Chem. Lett. 3 (2012) 735−743

[16] G. Debenedetti, Metastable Liquids: Concepts and Principles, Princeton University Press 1997

[17] I.S. Gutzow, J.W.P. Schmelzer, The Vitreous State: Thermodynamics, Structure, Rheology, and Crystallization, Springer Berlin Heidelberg 2013

[18] G. Floudas, M. Paluch, A. Grzybowski, and K.L. Ngai, Molecular Dynamics of Glass-Forming Systems: Effects of Pressure, Springer Series Advances in Dielectrics, series edited by F. Kremer (Springer, Berlin, 2011)

[19] C.M. Roland, S. Hensel-Bielowka, M. Paluch, R. Casalini, Supercooled dynamics of glass-forming liquids and polymers under hydrostatic pressure. Rep. Prog. Phys. 68 (2005) 1405-1478

[20] K.L. Ngai, Relaxation and Diffusion in Complex Systems. Springer 2011

[21] P.J. Marsac, H. Konno, L.S. Taylor, A comparison of the physical stability of amorphous felodipine and nifedipine systems. Pharm. Res. 23 (2006) 2306–2316

[22] D. Zhou, D.J.W Grant, G.G.Z. Zhang, D. Law, E.A. Schmitt, Physical stability of amorphous pharmaceuticals: importance of configurational thermodynamic quantities and molecular mobility. J. Pharm. Sci. 91 (2002) 71–83.

[23] R. Laitinen, K. Lobmann, C. Strachan, H. Grohganz, T. Rades, Emerging trends in the stabilization of amorphous drugs. International Journal of Pharmaceutics, 453 (2013) 65-79

[24]A. M. Kaushal, A.K. Bansal, Thermodynamic behavior of glassy state of structurally related compounds. Eur. J. Pharm. Biopharm. 69 (2008) 1067–1076.

[25] K.A. Graeser, J.E. Patterson, J.A. Zeitler, K.C. Gordon, T. Rades, Correlating thermodynamic and kinetic parameters with amorphous stability. Eur. J. Pharm.Sci. 37 (2009) 492-498

[26] D. Zhou, D.J.W. Grant, G.G.Z. Zhang, D. Law, E.A. Schmitt, A calorimetric investigation of thermodynamic and molecular mobility contributions to the physical stability of two pharmaceutical glasses. J. Pharm. Sci. 96 (2007) 71–83.

[27] P. Gupta, G. Chawla, and A.K. Bansal,. Physical stability and solubility of advantage from amorphous celecoxib: the role of thermodynamic quantities and molecular mobility. Molecular Pharmaceutics, 1 (2004) 406-413.

[28] C. Bhugra, M.J. Pikal, Role of thermodynamic, molecular, and kinetic factors in crystallization from the amorphous state. J. Pharm. Sci. 97 (2008) 1329-1349

[29] S.L. Shamblin, X. Tang, L. Chang, B.C. Hancock, M.J. Pikal, Characterization of the time scales of molecular motion in pharmaceutically important glasses. J. Phys. Chem. B, 103 (1999) 4113-4121.

[30] S.L. Shamblin, B.C. Hancock, Y. Dupuis, M.J. Pikal, Interpretation of relaxation time constant for amorphous pharmaceutical systems. J. Pharm. Sci. 89 (2000) 417-427.

[31] B.C. Hancock, S.L. Shamblin, Molecular mobility of amorphous pharmaceuticals determined using differential scanning calorimetry. Thermochim. Acta, 380 (2001) 95-107.

[32] C.A. Angell, K.L. Ngai, G.B. McKenna, P.F. McMillan, and S.W. Martin, Relaxation in glassforming liquids and amorphous solids, J. Applied Physics 88 (2000) 3113-3157

[33] M. Paluch, A. Patkowski, and E. W. Fischer, Temperature and pressure scaling of the alpha relaxation process in fragile glass formers: a dynamic light scattering study, Phys. Rev. Lett. 85 (2000) 2140-2143

[34] M. Paluch, M. Sekula, S. Pawlus, S. J. Rzoska, J. Ziolo, and C. M. Roland, Test of the Einstein-Debye Relation in Supercooled Dibutylphthalate at Pressures up to1.4 GPa, Phys. Rev. Lett. 90 (2003) 175702-1-175702-4.

[35] M. Paluch, C. M. Roland, S. Pawlus, J. Zioło, and K. L. Ngai, Does the Arrhenius Temperature Dependence of the Johari-Goldstein Relaxation Persist above Tg? Phys. Rev. Lett. 91 (2003) 115701-1-115701-4.

[36] L. Hong, A.B. Begen, A. Kisliuk, S. Pawlus, M. Paluch, and A.P. Sokolov, Influence of Pressure on Quasielastic Scattering in Glasses: Relationship to the Boson Peak, Phys. Rev. Lett. 102 (2009) 145502-1-145502-4.

[37] Z. Wojnarowska, C.M. Roland, A. Swiety-Pospiech, K. Grzybowska, and M. Paluch, Anomalous Electrical Conductivity Behavior at Elevated Pressure in the Protic Ionic Liquid Procainamide Hydrochloride, Phys. Rev. Lett. 108, (2012) 015701-1-015701-4.

[38] N. K. Thakral, S. Mohapatra, G.A. Stephenson, R. Suryanarayanan, Compression-induced crystallization of amorphous indomethacin in tablets: characterization of spatial heterogeneity by two-dimensional X-ray diffractometry. Mol Pharm. 12 (2015) 253-63

[39] K. Adrjanowicz, A. Grzybowski, K. Grzybowska, J. Pionteck, M. Paluch, Toward Better Understanding Crystallization of Supercooled Liquids under Compression: Isochronal Crystallization Kinetics Approach, Cryst. Growth Des. 13 (2013) 4648 − 4654

[40] K. Adrjanowicz, A. Grzybowski, K. Grzybowska, J. Pionteck, M. Paluch, Effect of High Pressure on Crystallization Kinetics of van der Waals Liquid: An Experimental and Theoretical Study, Cryst. Growth Des. 14 (2014) 2097−2104

[41] K. Adrjanowicz, A. Grzybowski, K. Kaminski, M. Paluch, Temperature and Volume Effect on the Molecular Dynamics of Supercooled Ibuprofen at Ambient and Elevated Pressure, Mol. Pharmaceutics 8 (2011) 1975–1979

[42] F. Kremer, A. Schönhals, Broadband dielectric spectroscopy, Springer 2003

[43] G. Schaumburg, New broadband dielectric spectrometers, Dielectric Newsletter, Issue July (1994) 8-12

[44] G. Schaumburg, Overview: Modern measurements techniques in Broadband Dielectric Spectroscopy, Dielectric Newsletter, Issue March (1994) 4-7

[45] M. Tonouchi, Cutting-edge terahertz technogoly. Nature Photonics, 1 (2007) 97-105.

[46] J. Sibik, S.R. Elliott, J.A. Zeitler, Thermal Decoupling of Molecular-Relaxation Processes from the Vibrational Density of States at Terahertz Frequencies in Supercooled Hydrogen-Bonded Liquids, J. Phys. Chem. Lett. 5 (2014) 1968–1972.

[47] G. P. Johari, M. Goldstein, Viscous liquids and the glass transition. II. secondary relaxations in glasses of rigid molecules, J. Chem. Phys. 53 (1970) 2372-2388

[48] G. P. Johari, Localized molecular motions of beta-relaxation and its energy landscape, J. Non-Cryst. Solids 307 (2002) 317-325

[49] G. Williams, D.C. Watts, S.B. Dev, A.M. North, Further considerations of non symmetrical dielectric relaxation behaviour arising from a simple empirical decay function, Trans. Faraday Soc. 67 (1971) 1323-1335

[50] G. P. Johari, K. Pathmanathan, An analysis for β-process in several molecular glasses, J. Chem. Phys. 85 (1986) 6811-

[51] S. Hensel-Bielówka, M. Paluch, K. L. Ngai, Emergence of the genuine Johari–Goldstein secondary relaxation in m-fluoroaniline after suppression of hydrogen-bond-induced clusters by elevating temperature and pressure, J. Chem Phys. 123 (2005) 014502-1-9.

[52] K.L. Ngai, M. Paluch, Classification of secondary relaxation in glass-formers based on dynamic properties J. Chem. Phys. 120 (2004) 857-873

[53] W. Stockmayer, Dielectric dispersion in solutions of flexible polymers, Pure and Appl. Chem. 15 (1967) 539-554.

[54] S. Havriliak, S. Negami, A complex plane analysis of a-dispersions in some polymer systems. Polym. Sci. C 14 (1966) 99-117

[55] S. Havriliak, S. Negami, A complex plane representation of dielectric and mechanical relaxation processes in some polymers, Polymer 8 (1967) 161-210

[56] K. S. Cole, R. H. Cole, Dispersion and Absorption in Dielectrics I: Alternating Current Characteristics, J. Chem. Phys. 9 (1941) 341-351

[57] H. Vogel, Das Temperaturabhangigkeitgesetz der Viskosität von Flüssigkeiten. J. Phys. Z. 22 (1921) 645-646.

[58] G.S. Fulcher, Analysis of Recent Measurements of the Viscosity of Glasses. J. Am. Ceram. Soc.8 (1925) 339-355.

[59] G. Tammann, W. Hesse, Die Abhängigkeit der Viscosität von der Temperatur bie unterkühlten Flüssigkeiten. Z. Anorg. Allg. Chem. 156 (1926) 245-257.

[60] C.A. Angell, Why c1 = 16-17 in the WLF equation is physical - and the fragility of polymers, Polymer 38 (1997) 6261-6266.

[61] G. Adam, J.H. Gibbs, On the temperature dependence of cooperative relaxation properties in glass forming liquids. J. Chem. Phys. 43 (1965) 139-146.

[62] K. Grzybowska, A. Grzybowski, J. Ziolo, S. J. Rzoska, M. Paluch, Anomalous behavior of secondary dielectric relaxation in polypropylene glycols, J. Phys. Condens. Matter 19, 376105 (2007)

[63] C. Bhugra, R. Shmeis, S.L. Krill, M.J. Pikal, Prediction of Onset of Crystallization from Experimental Relaxation Times. II. Comparison between Predicted and Experimental Onset Times, J. Pharm. Sci. 97 (2008) 455-472

[64] V. Andronis, G. Zografi, Molecular mobility of supercooled amorphous indomethacin, determined by dynamic mechanical analysis. Pharm. Res. 14 (1997) 410–414

[65] A.K.R. Dantuluri , A. Amin , V. Puri , and A.K. Bansal. Role of α – relaxation on crystallization od amorphous celecoxib above Tg probed by dielectric spectroscopy, Mol. Pharmaceutics, 8 (2011) 814–822

[66] J. Knapik, Z. Wojnarowska, K. Grzybowska, L. Hawelek, W. Sawicki, K. Włodarski, J. Markowski, M. Paluch, Physical stability of the amorphous anticholesterol agent (ezetimibe): the role of molecular mobility, Mol.Pharmaceut., 11 (2014) 4280-4290

[67] D. Zhou, G.G.Z. Zhang, D. Law, D.J.W Grant, E.A. Schmitt, Thermodynamics, molecular mobility and crystallization kinetics of amorphous griseofulvin. Mol. Pharm. 5 (2008) 927–936

[68] S.P. Bhardwaj, K.K. Arora, E. Kwong, A. Templeton, S.D. Clas, R. Suryanarayanan, Correlation between molecular mobility and physical stability of amorphous itraconazole. Mol Pharm. 10 (2013) 694-700

[69] S. P. Bhardwaj, R. Suryanarayanan, Molecular Mobility as an Effective Predictor of the Physical Stability of Amorphous Trehalose, Molecular Pharmaceutics, Mol. Pharm.11 (2012) 3209-17

[70] C. A. Angell, Relaxation in liquids, polymers and plastic crystals – strong/fragile patterns and problems. J. Non-Cryst. Solids, 131-133 (1991) 13-31.

[71] Fragility of Glass-forming Liquids, Vol 13 of Series: Texts and Readings in the Physical Sciences, Eds: A. Lindsay Greer, Kenneth F. Kelton, Srikanth Sastry, Hindustan Book Agency, New Delhi, 2014

[72] R. Böhmer, K.L. Ngai, C.A. Angell, D. Plazek, J. Non-exponential relaxations in strong and fragile glass-formers. J. Chem. Phys. 1993, 99, 4201-4209.

[73] R. Casalini and C.M. Roland, Scaling of the supercooled dynamics and its relation to the pressure dependences of the dynamic crossover and the fragility of glass formers, Phys. Rev. B 71, 014210 (2005)

[74] C. Alba-Simionesco and G. Tarjus, Temperature versus density effects in glassforming liquids and polymers: A scaling hypothesis and its consequences, J. Non-Cryst. Solids 352 (2006) 4888-4894

[75] M. Paluch, K. Grzybowska, A. Grzybowski, Effect of high pressure on relaxation dynamics of glass forming liquids, J. Phys.: Condens. Matter 19 (2007) 205117-205128

[76] M. Paluch, E. Masiewicz, A. Grzybowski, S. Pawlus, J. Pionteck, Z. Wojnarowska, General rules prospected for the liquid fragility in various material groups and different thermodynamic condition , J. Chem. Phys. 141 (2014) 134507-1 - 134507-7

[77] G. Williams, Complex dielectric constant of dipolar compounds as a function of temperature, pressure and frequency. Part 1. General relations and a consideration of models for relaxation Trans. Faraday Soc. 60 (1964) 1548-1555

[78] M.D. Ediger, P. Harrowell, and L. Yu, Crystal growth kinetics exhibit a fragility-dependent decoupling from viscosity. J. Chem. Phys. 128, 034709 (2008)

[79] D.N. Perera, Compilation of the frafility parameters for several glass-forming metallic alloys. J. Phys. Condens. Matter 1999, 11, 3807-3812.

[80] Z.P. Lu, Y. Li, C.T. Liu, Glass-forming tendency of bulk La-Al-Ni-Cu-(Co) metallic glass-forming liquids. J. Appl. Phys. 93 (2003) 286-290.

[81] H. Tanaka, Relationship among glass-forming ability, fragility, and short-range bond ordering of liquids J. Non-Cryst. Solids, 351 (2005) 678-690.

[82] H. Shintani, H. Tanaka, Frustration on the way to crystallization in glass. Nature Phys. 2 (2006) 200-206.

[83] A.B. Joshi, S. Patel, A.M. Kaushal, A.K. Bansal, Compaction studies of alternate solid forms of celecoxib. Adv. Powder Technol. 21 (2010) 452 − 460.

[84] M. Rams-Baron, Z. Wojnarowska, K. Grzybowska, M. Dulski, J. Knapik, K. Jurkiewicz, W. Smolka, W. Sawicki, A. Ratuszna, M. Paluch, Towards a better understanding of the physical stability of amorphous anti-inflammatory agents: the role of molecular mobility and molecular interaction patterns, Mol. Pharm. (submitted)

[85] K. Grzybowska, M. Paluch, A. Grzybowski, S. Pawlus, S. Ancherbak, D. Prevosto, S. Capaccioli, Dynamic Crossover of Water Relaxation in Aqueous Mixtures: Effect of Pressure, J. Phys. Chem. Lett. 1 (2010) 1170–1175

[86] K. Kawakami, T. Harada, Y. Yoshihashi, E. Yonemochi, K. Terada, H. Moriyama, Correlation between Glass-Forming Ability and Fragility of Pharmaceutical Compounds, J. Phys. Chem. B, 119 (2015) 4873−4880

[87] J.A. Baird, B. van Eerdenbrugh, L.S. Taylor, A Classification System to Assess the Crystallization Tendency of Organic Molecules from Undercooled Melts, J. Pharm. Sci. 99 (2010) 3787-3806

[88] J.A. Baird, L.S. Taylor, Evaluation of amorphous solid dispersion properties using thermal analysis techniques, Advanced Drug Delivery Reviews 64 (2012) 396–421

[89] I. Gutzow, J. Schmelzer, The Vitreous State: Structure, Thermodynamics, Rheology and Crystallization; Springer-Verlag: Berlin, 1995

[90] K.J. Crowley, G. Zografi, The use of thermal methods for predicting glass-former fragility, Thermochim. Acta 380 (2001) 79–93.

[91] G.P. Johari, S. Kim, R. M. Shanker, Dielectric Studies of Molecular Motions in Amorphous Solid and Ultraviscous Acetaminophen, J. Pham. Sci. 94 (2005) 2207-2223

[92] A.R. Bras, J.P. Noronha, A.M.M. Antunes, M.M. Cardoso, A. Schonhals, F. Affouard, M. Dionisio, N.T. Correia, Molecular Motions in Amorphous Ibuprofen As Studied by Broadband Dielectric Spectroscopy. J. Phys. Chem. B 112 (2008) 11087−11099.

[93] K. Adrjanowicz, Z. Wojnarowska, P. Wlodarczyk, K. Kaminski, M. Paluch, J. Mazgalski, Molecular mobility in liquid and glassy states of Telmisartan (TEL) studied by Broadband Dielectric Spectroscopy. Eur. J. Pharm. Sci. 38 (2009) 395.

[94] A.R. Bras, J.P. Noronha, A.M.M. Antunes, M.M. Cardoso, A. Schonhals, F. Affouard, M. Dionisio, N.T. Correia, Molecular motions in amorphous Ibuprofen as studied by Broadband Dielectric Spectroscopy. J. Phys. Chem. B 112 (2008) 11087–11099.

[95] F. Stickel, E.W. Fischer, R. Richert, Dynamics of glass-forming liquids. I. Temperature-derivative analysis of dielectric relaxation data. J. Chem. Phys. 102 (1995) 6251-6257.

[96] G.P. Johari, S. Kim, R.M. Shanker, Dielectric relaxation and crystallization of ultraviscous melt and glassy states of Aspirin, Ibuprofen, Progesterone, and Quinidine. J. Pharm. Sci. 96 (2007) 1159–1175.

[97] G.P. Johari, S. Kim, Ravi M. Shanker, Dielectric Study of Equimolar Acetaminophen–Aspirin, Acetaminophen–Quinidine, and Benzoic Acid–Progesterone Molecular Alloys in the Glass and Ultraviscous States and Their Relevance to Solubility and Stability, J. Pharm. Sci. 99 (2010) 1358-1374

[98] G. Williams, and D.C. Watts, Non-symmetrical dielectric relaxation behaviour arising from a simple empirical decay function. Trans. Faraday Soc. 66 (1970) 80-85.

[99] E. Tombari, C. Ferrari, G.P. Johari, R.M. Shanker, Calorimetric relaxation in pharmaceutical molecular glasses and its utility in understanding their stability against crystallization, J. Phys. Chem. B. 112 (2008) 10806-10814.

[100] K. Kolodziejczyk, M. Paluch, K. Grzybowska, A. Grzybowski, Z. Wojnarowska, L. Hawelek, Relaxation Dynamics and Crystallization Study of Sildenafil in the Liquid and Glassy States, Mol. Pharmaceutics 10 (2013) 2270–2282

[101] C.M. Roland, S. Hensel-Bielowka, M. Paluch, R. Casalini, Supercooled dynamics of glass-forming liquids and polymers under hydrostatic pressure. Rep. Prog. Phys. 68 (2005) 1405-1478.

[102] K. L. Ngai, R. Casalini, S. Capaccioli, M. Paluch, and C. M. Roland, Do Theories of the Glass Transition, in which the Structural Relaxation Time Does Not Define the Dispersion of the Structural Relaxation, Need Revision? J. Phys. Chem. B 109 (2005) 17356–17360.

[103] I. Saika-Voivod, R.K. Bowles, P.H. Poole, Crystal Nucleation in a Supercooled Liquid with Glassy Dynamics. Phys. Rev. Lett. 103 (2009) 225701-1-4

[104] T. Kawasaki, T. Araki, H. Tanaka, Correlation between Dynamic Heterogeneity and Medium-Range Order in Two-Dimen-sional Glass-Forming Liquids. Phys. Rev. Lett. 99 (2007) 215701-1-4

[105] H. Tanaka, Relationship among glass-forming ability, fragility, and short-range bond ordering of liquids. J. Non-Cryst. Solids, 351 (2005) 678 – 690

[106] H. Shintani, H. Tanaka, Frustration on the way to crystallization in glass. Nat. Phys. 2 (2006) 200–206

[107] T. Kawasaki and H. Tanaka, Formation of a crystal nucleus from liquid. Proc. Natl. Acad. Sci. USA 107 (2010) 14036–14041;

[108] M. Leocmach and H. Tanaka, Roles of icosahedral and crystal-like order in the hard spheres glass transition. Nature Communications 3 (2012) 974-1- 974-1

[109] Dynamical Heterogeneities in Glasses, Colloids, and Granular Media, (Eds.: L. Berthier, G. Biroli, J.-P. Bouchaud, L. Cipelletti, and W. van Saarloos), International Series of Monographs on Physics, vol. 150, Oxford University Press, 2011

[110] L. Berthier, G. Biroli, J.-P. Bouchaud, L. Cipelletti, D. El Masri, D. L'Hôte, F. Ladieu, and M. Pierno, Direct Experimental Evidence of a Growing Length Scale Accompanying the Glass Transition, Science 310 (2005) 1797-1800

[111] C. Dalle-Ferrier, C. Thibierge, C. Alba-Simionesco, L. Berthier, G. Biroli, J.-P. Bouchaud, F. Ladieu, D. L'Hoˆte, and G. Tarjus, Spatial correlations in the dynamics of glassforming liquids: Experimental determination of their temperature dependence, Phys. Rev. E 76 (2007) 041510-15

[112] C.M. Roland, D. Fragiadakis, D. Coslovich, S. Capaccioli, and K.L. Ngai, Correlation of nonexponentiality with dynamic heterogeneity from four-point dynamic susceptibility $\chi 4(t)$ and its approximation $\chi T(t)$. J. Chem. Phys. 133 (2010) 124507-1 - 124507-4

[113] K. Koperwas, A. Grzybowski, K. Grzybowska, Z. Wojnarowska, A. P. Sokolov, M. Paluch, Effect of Temperature and Density Fluctuations on the Spatially Heterogeneous Dynamics of Glass-Forming Van der Waals Liquids under High Pressure, Phys. Rev. Lett. 111 (2013) 125701-1 - 125701-5

[114] E. Donth, The size of cooperatively rearranging regions at the glass transition, J. Non. Cryst. Solids, 53 (1982) 325-330

[115] E. Donth, The Glass Transition, Relaxation Dynamics in Liquids and Disordered Materials, Springer, Berlin, 2001

[116] A. Grzybowski, K. Kolodziejczyk, K. Koperwas, K. Grzybowska, M. Paluch, Effects of lowering temperature and raising pressure on the spatially heterogeneous dynamics of glass-forming van der Waals liquids, Phys. Rev. B 85 (2012) 220201(R)-1 - 220201(R)-5

[117] S. Vyazovkin, I. Dranca, Physical Stability and Relaxation of Amorphous Indomethacin. J. Phys. Chem. B. 109 (2005) 18637-18644

[118] K. Kawakami, Dynamics of Ribavirin Glass in the Sub-Tg Temperature Region, J. Phys. Chem. B, 115 (2011) 11375–11381

[119] A.A. Cabral, V.M. Fokin, E.D. Zanotto, C.R. Chinaglia, Nanocrystallization of fresnoite glass. I. Nucleation and growth kinetics, J. Non-Cryst. Solids 330 (2003) 174–186

[120] A. A. Abu-Sehly, Study of the kinetics of non-isothermal crystallization in Ge20Te80 chalcogenide glass, Physica B, 325 (2003) 372–379

[121] G. Aldica, M. Secu, Investigations of the non-isothermal crystallization of CaF2 nanoparticles in Sm-doped oxy-fluoride glasses, J. Non-Crys. Solids 356 (2010) 1631–1636

[122] J. Cai, Q. Yu, Y. Han, X. Zhan, L. Jiang, Thermal stability, crystallization, structure and morphology of syndiotactic 1,2-polybutadiene/organoclay nanocomposite, Eur. Polym J. 43 (2007) 2866–2881

[123] K. Kaminski, K. Adrjanowicz, Z. Wojnarowska, M. Dulski, R. Wrzalik, M. Paluch., E. Kamińska, A. Kasprzycka, Do Intermolecular Interactions Control Crystallization Abilities of Glass-Forming Liquids?, J Phys Chem B. 115 (2011) 11537-47.

[124] E. Puel, E. Verdurand, P. Taulelle, C. Bebon, D. Colson, J. P. Klein, S. Veesler, Crystallization mechanisms of acicular crystals, J. Cryst. Growth 310 (2008) 110–115

[125] K. Adrjanowicz, K. Kaminski, Z. Wojnarowska, M. Dulski, L. Hawelek, S. Pawlus, M. Paluch, W. Sawicki, Dielectric Relaxation and Crystallization Kinetics of Ibuprofen at Ambient and Elevated Pressure, J. Phys. Chem. B 114 (2010) 6579–6593

[126] I.M. Hodge, Strong and fragile liquids – a brief critique, J. Non-Cryst. Solids, 202 (1996) 164-172.

[127] K. Grzybowska, A. Grzybowski, S. Pawlus, J. Pionteck, and M. Paluch, Role of entropy in the thermodynamic evolution of the time scale of molecular dynamics near the glass transition. Phys. Rev. E 91 (2015) 062305-1 - 062305-13

[128] A. Grzybowski, M. Paluch, K. Grzybowska, and S. Haracz, Communication: Relationships between intermolecular potential, thermodynamics, and dynamic scaling in viscous systems, J. Chem. Phys. 133 (2010) 161101-1 - 161101-4

[129] K. Grzybowska, A. Grzybowski, J. Knapik, and M. Paluch. A total entropy based method for predicting the structural relaxation time scale in the glassy state: Pharmaceutical applications (submitted)

[130] K.L. Ngai, Correlation between the secondary β-relaxation time at Tg with the Kohlrausch exponent of the primary α relaxation or the fragility of glass-forming material, Phys. Rev. E, 57 (1998) 7346-7349.

[131] K.L. Ngai and S. Capaccioli, Relation between the activation energy of the Johari-Goldstein β relaxation and Tg of glass formers, Phys. Rev. E 69 (2004) 031501-1-5.

[132] Ngai, K. L. An extended coupling model description of the evolution of dynamics with time in supercooled liquids and ionic conductors. J. Phys. Condens. Matter, 15 (2003) S1107- S1125.

[133] R. Casalini, C.M. Roland, Aging of the Secondary Relaxation to Probe Structural Relaxation in the Glassy State, Phys. Rev. Lett. 102 (2009) 035701-1-4.

[134] K. Kaminski, K. Adrjanowicz, E. Kaminska, and M. Paluch, Probing of structural relaxation times in the glassy state of sucrose and trehalose based on dynamical properties of two secondary relaxation processes, Phys. Rev. E 83 (2011) 061502

[135] K. Adrjanowicz, Z. Wojnarowska, P. Wlodarczyk, K. Kaminski, M. Paluch, Mazgalski, Molecular mobility in liquid and glassy states of Telmisartan (TEL) studied by Broadband Dielectric Spectroscopy, J. European Journal of Pharmaceutical Sciences, 38 (2009) 395-404

[136] I. Gutzow, J. Schmelzer, The Vitreous State: Structure, Thermodynamics, Rheology and Crystallization; Springer-Verlag: Berlin, 1995

[137] G. Tarjus and D. Kivelson, Breakdown of the Stokes–Einstein relation in supercooled liquids. J. Chem. Phys. 103 (1995) 3071-3073

[138] K.L. Ngai, J.H. Magill, and D.J. Plazek. Flow, diffusion and crystallization of supercooled liquids: Revisited. J. Chem. Phys. 112 (2000) 1887-1892

[139] S.R. Becker, P.H. Poole, and F.W. Starr, Fractional Stokes-Einstein and Debye-Stokes-Einstein Relations in a Network-Forming Liquid. Phys. Rev. Lett. 97 (2006) 055901-1 - 055901-4

[140] K.R. Harris, The fractional Stokes–Einstein equation: Application to Lennard-Jones, molecular, and ionic liquids. J. Chem. Phys. 131 (2009) 054503-1 - 054503-8

[141] K.V. Edmond, M.T. Elsesser, G.L. Hunter, D.J. Pine, and E.R. Weeks, Decoupling of rotational and translational diffusion in supercooled colloidal fluids. Proc. Natl. Acad. Sci. USA, 44 (2012) 17891–17896

[142] D.A. Turton and K. Wynne, Stokes − Einstein − Debye Failure in Molecular Orientational Diffusion: Exception or Rule? J. Phys. Chem. B, 118 (2014) 4600−4604

[143] N.B. Olsen, J.C. Dyre, and T. Christensen, Structural Relaxation Monitored by Instantaneous Shear Modulus. Phys. Rev. Lett. 81 (1998) 1031-1033

[144] L. Carpentier, R. Decressain, S. Desprez, and M. Descamps, Dynamics of the Amorphous and Crystalline α-, γ-Phases of Indomethacin. J. Phys. Chem. B 110 (2006) 457-464

[145] K. Kothari, V. Ragoonanan, R. Suryanarayanan, The Role of Polymer Concentration on the Molecular Mobility and Physical Stability of Nifedipine Solid Dispersions, Mol. Pharmaceutics, 12 (2015) 1477−1484

[146] V. Caron, C. Bhugra, M. J. Pikal, Prediction of Onset of Crystallization in Amorphous Pharmaceutical Systems: Phenobarbital, Nifedipine/PVP, and Phenobarbital/PVP, J. Pharm. Sci. 99 (2010) 3887-3900

[147] S. Bhattacharya, R. Suryanarayanan, Local mobility in amorphous pharmaceuticals-characterization and implications on stability, J. Pharm. Sci. 98 (2009) 2935–2953.

[148] K. L. Ngai, K. Y. Tsang, Similarity of relaxation in supercooled liquids and interacting arrays of oscillators Phys. Rev. E 60 (1999) 4511-4517

[149] K. Nelson, American Chemical Society, Washington DC, Chap. 4, p. 45 (1997)

[150] K. L. Ngai, R. W. Rendell, in Supercooled Liquids: Advances and Novel Applications, ACS Symposium Series Vol. 676, edited by J. T. Fourkas, D. Kivelson, U. Mohanty

[151] T. Hikima, M. Hanaya, M. Oguni, β-molecular rearrangement process, but not an α-process, as governing the homogeneous crystal-nucleation rate in a supercooled liquid. Bull. Chem. Soc. Jpn., 69 (1996) 1863-1868

[152] T. Hikima, M. Hanaya, M. Oguni, Microscopic observation of a peculiar crystallization in the glass transition region and β-process as potentially controlling the growth rate in triphenylethylene. J. Mol. Struct., 479 (1999) 245-250

[153] N. Okamoto, M. Oguni, Discovery of crystal nucleation proceeding much below the glass transition temperature in a supercooled liquid. Solid State Commun. 99 (1996) 53–56

[154] F. Paladi, M. Oguni, Anomalous generation and extinction of crystal nuclei in nonequilibrium supercooled liquid o-benzylphenol. Phys. Rev. B. 65 (2002) 144202-144207

[155] F. Paladi, M. Oguni, J. Phys.: Generation and extinction of crystal nuclei in an extremely non-equilibrium glassy state of salol. Condens. Matter 15 (2003) 3909-3917

[156] M. Hatase, M. Hanaya, T. Hikima, M. Oguni, Discovery of homogeneous-nucleation-based crystallization in simple glass-forming liquid of toluene below its glass-transition temperature. J. Non-Cryst. Solids 307-310 (2003) 257-263

[157] S. Tomitaka, M. Muzukami, F. Paladi, M. Oguni, Thermal and dielectric studies of 2,2'-dihydroxybenzophenone, J. Therm. Anal. 81 (2005) 637–643.

[158] Y. Sun, H. Xi, M. D. Ediger, R. Richert, and L. Yu, Diffusion-controlled and "diffusionless" crystal growth near the glass transition temperature: Relation between liquid dynamics and growth kinetics of seven ROY polymorphs. J. Chem. Phys. 131 (2009) 074506-1 - 074506-9

[159] H. Xi, Y. Sun, L. Yu, Diffusion-controlled and diffusionless crystal growth in liquid o -terphenyl near its glass transition temperature, J. Chem. Phys. 130 (2009) 094508-1 - 094508-9

[160] H. Fujimori, M. Oguni, Correlation index (Tga-Tgb)/Tga and activation energy ration as parameters characterizing the structure of liquid and glass. Solid State Commun.94, 157-162 (1995)

[161] H. Wagner and R. Richert, Equilibrium and Non-Equilibrium Type β-Relaxations: D-Sorbitol versus o-Terphenyl. J. Phys. Chem. B 103 (1999) 4071 - 4077

[162] J. Sibik, S.R. Elliott, and J. A. Zeitler, Thermal Decoupling of Molecular-Relaxation Processes from the Vibrational Density of States at Terahertz Frequencies in Supercooled Hydrogen-Bonded Liquids, J. Phys. Chem. Lett. 5(2014) 1968 − 1972

[163] J. Sibik, K. Löbmann, T. Rades, J.A. Zeitler, Predicting Crystallization of Amorphous Drugs with Terahertz Spectroscopy, Mol. Pharmaceutics 12 (2015) 3062−3068.

[164] S. Capaccioli, K L. Ngai, M. Shahin Thayyil, and D. Prevosto, Coupling of Caged Molecule Dynamics to JG β‑ Relaxation: I. J. Phys. Chem. B, 119 (2015) 8800−8808

[165] S. Vyazovkin and I. Dranca, Effect of Physical Aging on Nucleation of Amorphous Indomethacin. J. Phys. Chem. B 111 (2007) 7283-7287

[166] L. Carpentier, R. Decressain, S. Desprez, and M. Descamps, Dynamics of the Amorphous and Crystalline α-, γ-Phases of Indomethacin. J. Phys. Chem. B 110 (2006) 457-464

[167] Z. Wojnarowska, K. Adrjanowicz, P. Wlodarczyk, E. Kaminska, K. Kaminski, K. Grzybowska, R. Wrzalik, M. Paluch, and K. L. Ngai, Broadband Dielectric Relaxation Study at Ambient and Elevated Pressure of Molecular Dynamics of Pharmaceutical: Indomethacin. J. Phys. Chem. B 113 (2009) 12536–12545

[168] Z. Wojnarowska, K. Grzybowska, L. Hawelek, A. Swiety-Pospiech, E. Masiewicz, M. Paluch, W. Sawicki, A. Chmielewska, P. Bujak, and J. Markowski, Molecular Dynamics Studies on the Water Mixtures of Pharmaceutically Important Ionic Liquid Lidocaine HCl, Mol. Pharmaceutics, 9 (2012) 1250−1261

[169] S.P. Duddu, T.D. Sokoloski, Dielectric analysis in the characterization of amorphous pharmaceutical solids. 1. Molecular mobility in poly(vinylpyrrolidone)–water systems in the glassy state. J. Pharm. Sci. 84 (1995) 773-776

[170] M. Gordon, J.S. Taylor, Ideal copolymers and the second-order transitions of synthetic rubbers 1: Non-crystalline copolymers. J. Appl. Chem., 2 (1952) 493-498.

[171] P.R. Couchman, F.E. Karasz, A classical thermodynamic discussion on the effect of composition on glass-transition temperatures. Macromolecules 11 (1978) 117-119.

[172] T. Miyazaki, S. Yoshioka, Y. Aso, S. Kojima, Ability of polyvinylpyrrolidone and polyacrylic acid to inhibit the crystallization of amorphous acetaminophen, J. Pharm. Sci., 93 (2004) 2710−2717.

[173] K. Khougaz, S.-D. Clas, Crystallization inhibition in solid dispersions of MK-0591 and poly(vinylpyrrolidone) polymers, J. Pharm. Sci. 89 (2000) 1325 - 1334.

[174] P. Gupta, R. Thilagavathi, A.K. Chakraborti, A.K. Bansal, Role of Molecular Interaction in Stability of Celecoxib−PVP Amorphous Systems, Mol. Pharm., 2 (2005) 384-391

[175] P. Mistry, S. Mohapatra, T. Gopinath, F.G. Vogt, R. Suryanarayanan, Role of the Strength of Drug − Polymer Interactions on the Molecular Mobility and Crystallization Inhibition in Ketoconazole Solid Dispersions, Mol. Pharmaceutics (2015) doi: 10.1021/acs.molpharmaceut.5b00333.

[176] L.A. Wegiel, L.J. Mauer, K.J. Edgar, L.S. Taylor, Mid-Infrared Spectroscopy as a Polymer Selection Tool for Formulating Amorphous Solid Dispersions, J. Pharm. Pharmacol., 66 (2014) 244−255.

[177] B. Van Eerdenbrugh, L.S. Taylor, An Ab Initiopolymer Selection Methodology to Prevent Crystallization in Amorphous Solid Dispersions by Application of Crystal Engineering Principles, Cryst.Eng.Comm., 13 (2011), 6171 − 6178.

[178] B. Van Eerdenbrugh, L.S. Taylor, Small-Scale Screening To Determine the Ability of Different Polymers to Inhibit Drug Crystallization Upon Rapid Solvent Evaporation. Mol. Pharmaceutics, 7 (2010) 1328−1337.

[179] T. Miyazaki, S. Yoshioka, Y. Aso, S. Kojima, Ability of Polyvinylpyrrolidone and Polyacrylic Acid To Inhibit the Crystallization of Amorphous Acetaminophen. J. Pharm. Sci., 93 (2004) 2710 − 2717.

[180] T. Matsumoto, G. Zografi, Physical Properties of Solid Molecular Dispersions of Indomethacin with Poly(vinylpyrrolidone) and Poly(vinylpyrrolidone-co-vinyl-acetate) in Relation to Indomethacin Crystallization. Pharm. Res., 16 (1999) 1722 − 1728.

[181] H. Konno, L.S. Taylor, Influence of Different Polymers on the Crystallization Tendency of Molecularly Dispersed Amorphous Felodipine. J. Pharm. Sci., 95 (2006) 2692 − 2705.

[182] K. Kothari, V. Ragoonanan, R. Suryanarayanan, The Role of Drug − Polymer Hydrogen Bonding Interactions on the Molecular Mobility and Physical Stability of Nifedipine Solid Dispersions. Mol. Pharmaceutics, 12 (2015) 162 − 170.

[183] P. Gupta, R. Thilagavathi, A.K. Chakraborti, A. K. Bansal, Role of Molecular Interaction in Stability of Celecoxib − PVP Amorphous Systems, Mol. Pharm. 2, (2005) 384-391

[184] P. Gupta, V. K. Kakumanu, A. K. Bansal Stability and Solubility of Celecoxib–PVP Amorphous Dispersions: A Molecular Perspective, Pharm. Res., 21, (2004) 1762-1769.

[185] E. Kaminska, K. Adrjanowicz, M. Tarnacka, K. Kolodziejczyk, M. Dulski, E.U. Mapesa, D. Zakowiecki, L. Hawelek, I. Kaczmarczyk-Sedlak, K. Kaminski, Impact of inter- and intramolecular interactions on the physical stability of indomethacin dispersed in acetylated saccharides, Mol. Pharm. 11 (2014) 2935-2947.

[186] E. Kaminska, M. Tarnacka, P. Wlodarczyk, K.Jurkiewicz, K. Kolodziejczyk, M. Dulski, D. Haznar-Garbacz, L. Hawelek, K. Kaminski, A. Wlodarczyk, M. Paluch, Studying the Impact of Modified Saccharides on the Molecular Dynamics and Crystallization Tendencies of Model API Nifedipine, Mol. Pharm. 12 (2015) 3007-3019.

[187] H. Liu, X. Zhang, H. Suwardie, P. Wang, C.G. Gogos, Miscibility studies of indomethacin and Eudragit(R) E PO by thermal, rheological, and spectroscopic analysis. J. Pharm. Sci., 101 (2012) 2204 − 2212.

[188] M.K. Gupta, A. Vanwert, R.H. Bogner, Formation of physically stable amorphous drugs by milling with Neusilin. J. Pharm. Sci., 92 (2003) 536 − 551.

[189] D. Bahl, R.H. Bogner, Amorphization of indomethacin by cogrinding with Neusilin US2: Amorphization kinetics, physical stability, and mechanism., Pharm. Res., 23 (2006) 2317 − 2325.

[190] J. Maclean, C. Medina, D. Daurio, F. Alvarez-Nunez, J. Jona, E. Munson, K. Nagapudi, Manufacture and performance evaluation of a stable amorphous complex of an acidic drug molecule and Neusilin. J. Pharm. Sci., 100 (2011) 3332 − 3344.

[191] S. Mallick, S. Pattnaik, K. Swain, P.K. De, A. Saha, G. Ghoshal, A. Mondal, A. Formation of physically stable amorphous phase of ibuprofen by solid-state milling with kaolin. Eur. J. Pharm. Biopharm., 68 (2008) 346−351.

[192] I. Weuts, D. Kempen, G. Verreck, J. Peeters, M. Brewster, N. Blaton, G. Van den Mooter, Salt formation in solid dispersions consisting of polyacrylic acid as a carrier and three basic model compounds resulting in very high glass transition temperatures and constant dissolution properties upon storage, Eur. J. Pharm. Sci., 25 (2005) 387 − 393.

[193] S.U. Yoo, S.L. Krill, Z. Wang, C. Telang, Miscibility/stability considerations in binary solid dispersion systems composed of functional excipients towards the design of multicomponent amorphous systems. J. Pharm. Sci., 98 (2009) 4711 − 4723.

[194] L.A. Wegiel, L.J. Mauer, K.J. Edgar, L.S. Taylor, Crystallization of amorphous solid dispersions of resveratrol during preparation and storage Impact of different polymers. J. Pharm. Sci., 102 (2013) 171 − 184.

[195] A.L. Sarode, H. Sandhu, N. Shah, W. Malick, H. Zia, Hot melt extrusion for amorphous solid dispersions: Temperature and moisture activated drug − polymer interactions for enhanced stability. Mol. Pharmaceutics, 10 (2013) 3665 − 3675.

[196] S. Yamamura, M. Momose, K. Takahashi, S. Nagatani, Solid-state interaction between cimetidine and naproxen, Drug Stability., 50 (1996) 173-178.

[197] S. Yamamura, H. Gotoh, Y. Sakamoto, Y. Momose, Physicochemical properties of amorphous precipitates of cimetidine-indomethacin binary system. Eur. J. Pharm. Biopharm., 49 (2000) 259–265.

[198] M. Allesø, N. Chieng, S. Rehder, J. Rantanen, T. Rades, J. Aaltonen, Enhanced dissolution rate and synchronized release of drugs in binary systems through formulation: Amorphous naproxen-cimetidine mixtures prepared by mechanical activation. J. Controlled Release, 136 (2009) 45–53.

[199] N. Chieng, J. Aaltonen, D. Saville, T. Rades, Physical characterization and stability of amorphous indomethacin and ranitidine hydrochloride binary systems prepared by mechanical activation. Eur. J. Pharm. Biopharm., 71 (2009) 47–54.

[200] K. Lobmann, R. Laitinen, H. Grohganz, K.C. Gordon, C. Strachan, T. Rades, Coamorphous Drug Systems: Enhanced Physical Stability and Dissolution Rate of Indomethacin and Naproxen. Mol. Pharmaceutics, 8 (2011) 1919–1928.

[201] K. Lobmann, C. Strachan, H. Grohganz, T. Rades, O. Korhonen, R. Laitinen, Co-amorphous simvastatin and glipizide combinations show improved physical stability without evidence of intermolecular interactions. Eur. J. Pharm. Biopharm., 81 (2012) 159-169.

[202] L.M. Martínez, M. Videa, G.A. López-Silva, C.A. de Los Reyes, J. Cruz-Angeles, N. González, Stabilization of amorphous paracetamol based systems using traditional and novel strategie, Int. J. Pharm., 477 (2014) 294-305.

[203] J. Knapik, Z. Wojnarowska, K. Grzybowska, K. Jurkiewicz, L. Tajber, and M. Paluch, Molecular dynamics and physical stability of co-amorphous ezetimib and indapamide mixtures Mol. Pharmaceutics 2015 (just accepted)

[204] Y. Du, X. Zhang, H. Ji, H. Liu, S. Li, L. Li, Probucol and atorvastatin in combination protect rat brains in MCAO model: Upregulating Peroxiredoxin2, Foxo3a and Nrf2 expression. Neuroscience Letters, 509 (2012) 110-115.

[205] T. Dyke, L. Litkowski, T. Kiersch, N. Zarringhalam, H. Zheng, K. Newman, Combination Oxycodone 5 mg/Ibuprofen 400 mg for the Treatment of Postoperative Pain: A Double-Blind, Placebo and Active-Controlled Parallel-Group Study. Clinical Therapeutics, 26 (2004) 2003-2014.

[206] J. Mao, Y. Zhang, J. Zhu, G. Zhang, Z. Guo, Molecular combo of photodynamic therapeutic agent silicon (IV) phthalocyanine and anticancer drug cisplatin, Chem. Commun., 8 (2009) 908-910.

[207] M.A. Neumann, J. van de Streek, F.P.A. Fabbiani, P. Hidber, O. Grassmann, Combined crystal structure prediction and high-pressure crystallization in rational pharmaceutical polymorph screening, Nature Communications 6:7793 (2015) DOI: 10.1038/ncomms8793

[208] R. Ceolin, J.L. Tamarit, M. Barrio, D. Lopez, B. Nicolai, N. Veglio, M.A: Perrin, P. Espeau, Overall Monotropic Behavior of a Metastable Phase of Biclotymol, 2,20-Methylenebis(4-Chloro-3-Methyl-Isopropylphenol), Inferred From Experimental and Topological Construction of the Related P-T State Diagram, J. Pharm. Science, 97 (2008) 3927

[209] K. Imamura, M. Nomura, K. Tanaka, N. Kataoka, J. Oshitani, H. Imanaka, K. Nakanishi, Impacts of Compression on Crystallization Behavior of Freeze-Dried Amorphous Sucrose, Journal of Pharmaceutical Sciences, Vol. 99 (2010) 1452–1463

[210] N. Mahe, M.A.Perrin, M. Barrio,B. Nicolai, I.B. Rietveld, J.L. Tamarit, R. Ceolin, Solid-State Studies of the Triclinic (Z' = 2) Antiprotozoal Drug Ternidazole, J. Pharm. Sci., 100 (2011) 2258–2266

[211] A. Sorrentino, R. Pantani, and G. Titomanlio, Crystallization of Syndiotactic Polystyrene under High Pressure and Cooling Rate, Macromolecular Research, 18 (2010) 1045-1052

[212] C. Grigoriadis, N. Haase, H.-J. Butt, K. Mullen, G. Floudas, To tilt or not to tilt? Kinetics of structure formation in a discotic liquid crystal, Soft Matter, 7 (2011) 4680

[213] M. Avrami, Kinetics of Phase Change. I General Theory. J. Chem. Phys. 7 (1939) 1103.

[214] M. Avrami, Kinetics of Phase Change. II Transformation-Time Relations for Random Distribution of Nuclei. *J. Chem. Phys*. 8 (1940) 212.

[215] S. Capaccioli, W. Tu, L.M. Wang (in preparation)

[216] K. Adrjanowicz, K. Kaminski, M. Paluch, K. L. Ngai, and Lian Yu, Study of dynamics and crystallization kinetics of 5-methyl-2-[(2-nitrophenyl)amino]-3-thiophenecarbonitrile at ambient and elevated pressure J. Chem. Phys. 136 (2012) 234509

[217] K. Adrjanowicz, K. Kaminski, M. Paluch, K. Niss, Crystallization Behavior and Relaxation Dynamics of Supercooled S-Ketoprofen and the Racemic Mixture along an Isochrone, Cryst. Growth Des.,15 (2015) 3257−3263

[218] K. Kessairi, S. Capaccioli, D. Prevosto, M. Lucchesi, S Sharifi, P.A. Rolla, Interdependence of Primary and Johari−Goldstein Secondary Relaxations in Glass-Forming Systems. J. Phys. Chem. B, 112 (2008) 4470−4473.

[219] M. Mierzwa, S. Pawlus, M. Paluch, E. Kaminska, K.L. Ngai, Correlation between Primary and Secondary Johari−Goldstein Relaxations in Supercooled Liquids: Invariance to Changes in Thermodynamic Conditions. J. Chem. Phys., 128 (2008) 044512

[220] T.S. Ingebrigtsen, T.B. Schrøder, J.C. Dyre, What Is a Simple Liquid? Phys. Rev. X, 2 (2012) 011011

[221] I. Gutzow, D. Durschang, C.J. Rüssel, Crystallization of glassforming melts under hydrostatic pressure and shear stress. Part I. Crystallization catalysis under hydrostatic pressure: possibilities and limitations. 32 (1997) 5389–5403

[222] I. Gutzow, C.J. Rüssel, D. Durschang, Crystallization of glassforming melts under hydrostatic pressure and shear stress. Part II. Flow induced melt crystallization: a new method of nucleation catalysis. 32 (1997) 5405 - 5411

[223] P. G. Tait, *Physics and Chemistry of the Voyage of H. M. S. Challenger* Vol. 2, Part 4 (HMSO, London, 1888)

[224] A. Grzybowski, K. Grzybowska, M. Paluch, A. Swiety, K. Koperwas, Density scaling in viscous systems near the glass transition, Phys. Rev. E, 83 (2011) 041505-1 - 041505-7

[225] A. Grzybowski, S. Haracz, M. Paluch, K. Grzybowska, *Density Scaling of Supercooled Simple Liquids Near the Glass Transition*, J. Phys. Chem. B, 114 (2010) 11544–11551

[226] A. Grzybowski, M. Paluch, K. Grzybowska, *Consequences of an Equation of State in the Thermodynamic Scaling Regime*, J. Phys. Chem. B, 113 (2009) 7419–7422

[227] T. Konishi, H.Tanaka, Possible origin of enhanced crystal growth in a glass, Phys. Rev. B, 76 (2007) 220201-1-4